

Review

Current Challenges and Innovative Developments in Hydroxyapatite-Based Coatings on Metallic Materials for Bone Implantation: A Review

Bilal Beig¹, Usman Liaqat^{1,*} , Muhammad Farooq Khan Niazi¹, Inamullah Douna¹ ,
Muhammad Zahoor² and Muhammad Bilal Khan Niazi¹ 

¹ School of Chemical and Materials Engineering, National University of Sciences and Technology (NUST), Islamabad 44000, Pakistan; bilal_beig@yahoo.com (B.B.); mfarooq.me09@scme.nust.edu.pk (M.F.K.N.); inamullah.che6@scme.nust.edu.pk (I.D.); m.b.k.niazi@scme.nust.edu.pk (M.B.K.N.)

² Department of Molecular Medicine, Institute of Basic Medical Sciences, University of Oslo, Sognsvannsveien 9, 0768 Oslo, Norway; muhammad.zahoor@medisin.uio.no

* Correspondence: usman.liaqat@scme.nust.edu.pk; Tel.: +92-51-90855223

Received: 20 October 2020; Accepted: 1 December 2020; Published: 18 December 2020



Abstract: Biomaterials are in use for the replacement and reconstruction of several tissues and organs as treatment and enhancement. Metallic, organic, and composites are some of the common materials currently in practice. Metallic materials contribute a big share of their mechanical strength and resistance to corrosion properties, while organic polymeric materials stand high due to their biocompatibility, biodegradability, and natural availability. To enhance the biocompatibility of these metals and alloys, coatings are frequently applied. Organic polymeric materials and ceramics are extensively utilized for this purpose due to their outstanding characteristics of biocompatibility and biodegradability. Hydroxyapatite (HAp) is the material from the ceramic class which is an ultimate candidate for coating on these metals for biomedical applications. HAp possesses similar chemical and structural characteristics to normal human bone. Due to the bioactivity and biocompatibility of HAp, it is used for bone implants for regenerating bone tissues. This review covers an extensive study of the development of HAp coatings specifically for the orthopaedic applications that include different coating techniques and the process parameters of these coating techniques. Additionally, the future direction and challenges have been also discussed briefly in this review, including the coating of HAp in combination with other calcium magnesium phosphates that occur naturally in human bone.

Keywords: hydroxyapatite; coating techniques; metallic biomaterials; current challenges; innovative method

1. Introduction

Titanium, stainless steel 316L, nickel-titanium, magnesium, and cobalt based metal alloys are broadly applied as orthopedic implants [1]. This is because of their higher mechanical strength, stability with wear, and corrosion resistance properties. The mechanical properties, advantages, and disadvantages associated with metallic implants are as shown in Table 1. On the other hand, all these metals or alloys, except magnesium, are considered biologically inert materials. Magnesium based alloys are considered to be as bioactive, biodegradable, and biotolerant for tissue engineering [2]. These metals and alloys are normally shaped as fracture plates, bones, hip nails, pins, wires, joint caps, and screws [3]. These implants are placed to hold the bones in place and help to promote osseointegration with bone tissue. Implants, used for tissue support, must be biocompatible and give clues to host cells to start a quick natural cell healing process [4]. Coatings on biomedical

implants are considered as a promising technique to enhance the implant-tissue interactions and promote their biocompatibility and biofunctionality without altering the material's properties [5,6]. Hydroxyapatite (HAp), calcium phosphate salts, and bio-active glasses are frequently used as a coating material. These materials come under the class of ceramics and possess superior chemical compatibility with physiological medium and stiff tissues, such as bones and teeth [7]. Additionally, these materials except bioactive glass show chemical and structural similarity with biological apatite [8,9]. There are different methods for the synthesis of HAp and the most common method is using pre-cursor hydrated calcium phosphate compound [10]. Werner was the first to name HAp in 1786 as a mineral. HAp is present abundantly on earth as a naturally occurring phosphatic compound. HAp has a very close link with natural bone in terms of composition and chemical formula. It is crystalline in nature with a density of 3.22 g/cm³. Each unit cell of HAp consists of Ca, PO₄, and OH ions which are closely packed to form the apatite structure [11]. Carbonated calcium-deficient HAp is a major part of dental enamel and dentin [12]. Hydroxyapatite contains calcium and phosphorus in a molar ratio of 1.67. This solid apatite is mainly stable due to calcium phosphate salt at ambient conditions and a wide range of pH ranging from 4 to 12. The HAp properties vary greatly with the change of chemical composition, crystallinity, size, and shape of the HAp crystals [13,14]. HAp nanoparticles possess excellent mechanical properties along with higher activity and resorb ability in comparison with bulk HAp [15]. This is because of the higher surface energy possesses by HAp nanoparticles [16]. These and other important properties make HAp the most important candidate for the coating of orthopedic implants.

Table 1. Mechanical properties, advantage and disadvantage of metallic implants [17,18].

Metals	Density (g/cm ³)	Elastic Modulus (Gpa)	Advantage	Disadvantage
Stainless steel 316 L	8	193	<ul style="list-style-type: none"> • Good corrosion and wear resistance 	<ul style="list-style-type: none"> • High Elastic modulus • Hinder bone regeneration due to high modulus
Titanium (Ti-6Al-4V)	4.4	110	<ul style="list-style-type: none"> • Higher biocompatibility and osseointegration in comparison to others • Excellent tensile strength, fracture toughness, and fatigue stress 	<ul style="list-style-type: none"> • Cytotoxic due to the presence of V and Al • Low corrosion and wear properties as compared to other metals but superior than Mg • Higher in cost
Co-Cr alloys	9.2	210	<ul style="list-style-type: none"> • Highest strength among all the metallic implants 	<ul style="list-style-type: none"> • Cytotoxic due to Co, Cr, and Ni • Low corrosion, wear and friction resistance
Mg	1.74	41–45	<ul style="list-style-type: none"> • Posseses similar properties like natural bone • Minimize stress shielding effect • Easy to synthesize into complex shapes • Light weight to support for load bearing applications • Mg²⁺ ions essential for human metabolism & provide stimulatory effects for bone regeneration 	<ul style="list-style-type: none"> • Very low corrosion resistance • Release of hydrogen gas • Premature loss of mechanical strength

HAp can be coated on metallic implants using various coating techniques [19]. The non-bioactivity factor of metals can be easily compensated by using HAp. The metallic implant with HAp coating supports new bone development due to strong interface between the coating and host tissue [20]. Additionally, HAp coating also acts as a corrosion control film against aggressive body fluids. This HAp film also retards the dissolution rate of metallic ions thus minimizing chances of leaching [21]. Several coating methods are available for the deposition of HAp on metallic implants. These methods include sol-gel, dip coating, electrochemical deposition, chemical vapor deposition, thermal spraying, radio frequency (RF) magnetron sputtering, micro-arc oxidation (MAO), high-velocity suspension flame spraying (HVSFS), plasma spraying, and pulsed laser deposition (PLD) [22]. Thermal spray coating is the most efficient and commonly applied nowadays on metallic implants due to its uniform coating layer on the metal surfaces [23].

The major concern during the coating process of HAp is the poor binding of HAp on the metallic surface. This is due to the low adhesive bond between metallic load-bearing sites and HAp film [24]. HAp film linkage on the metallic surface starts to reduce and suddenly fails, due to the poor crystalline nature of HAp [25]. This failure results in the discharge of metallic ions as the metal surface starts to expose against the body environment [26]. To enhance the adhesion of HAp films, surface modifying agents are required, which assist in the formation of durable film over the metallic surface. HAp is the major inorganic ingredient of hard tissues (bones) and has been applied in biomedical applications for the last 50 years due to its biocompatibility. On the other hand, previously reported studies revealed that HAp offers the properties of ceramics that are brittle and unable to withstand load [27]. As a result of previous studies, HAp was selected as a bioactive coating material for enhancement of mechanical properties. This coating supports the damaged tissue to heal quickly due to its bioactivity [28]. Few research studies have been carried out using a mixer of HAp and other mineral compounds to form composite materials with better mechanical strength [29]. Witte et al. developed a metallic composite using AZ91 magnesium alloy with HAp particle as reinforced filler in a metallic matrix [30]. Mechanical properties of composite materials are highly dependent on HAp particle size. The chitosan (CS) blend with HAp is also examined for biomedical applications. The majority of the research has been carried out to check the adhesive bond between HAp/CS film and metallic surface. The HAp/CS film is much stronger as compared to a single HAp film. The composite coating offers more bioactivity and biocompatibility than HAp film due to the presence of active agent calcium silicate which generates porosity with HAp on film surface [31].

The pros and cons of different techniques used for HAp coating on metallic bio-implants are depicted in Table 2. Conversely, this detailed article covers the regularly used technologies for HAp coating. These coating methods include sol-gel, dip coating, electrodeposition, plasma spraying, chemical vapor deposition, and pulsed laser deposition. This review thoroughly explains the raw materials, coating methods, thickness, and process parameters used in the above-said coating techniques.

Table 2. Pros and Cons of Different Coating Techniques.

Methods	Coating Layer Thickness	Pros	Cons	References
Sol-Gel	<1 μm	<ul style="list-style-type: none"> • Mild reaction conditions • Cheap method • Smooth coating layer • Higher purity of coating film • Easily process complicated structures 	<ul style="list-style-type: none"> • Few reactions need closed environment • Requires costly chemicals 	[32–38]

Table 2. Cont.

Methods	Coating Layer Thickness	Pros	Cons	References
Dip coating	0.05–15 mm	<ul style="list-style-type: none"> Cheap Easy to apply Easily process for complicated structures Uniform Coating Layer 	<ul style="list-style-type: none"> Requires high finishing temperature High temperature damages coating film 	[39–47]
Electro-chemical deposition	0.05–0.5 mm	<ul style="list-style-type: none"> Economical process Easy process for complicated substrates Uniformity of coating film 	<ul style="list-style-type: none"> Weak bonding between HAp film and metallic surface 	[48–51]
Electro-phoretic deposition	0.1–2.0 mm	<ul style="list-style-type: none"> Uniformity of coating layer Easy coating process for complicated substrate Coating rate is high 	<ul style="list-style-type: none"> Post treatment of coating at higher temperature Cracks develop at low temperatures 	[52–55]
Bio-mimetic coating	<30 μm	<ul style="list-style-type: none"> Lower reaction temperature Easily process complex shapes 	<ul style="list-style-type: none"> Time taking process Needs constant pH system Require solution makeup 	[56]
Plasma spraying	<20 μm	<ul style="list-style-type: none"> Low-cost process Fast coating Smooth coating layer Interconnected pores for multilayer coatings 	<ul style="list-style-type: none"> HAp film density fluctuates that effects uniformity Expensive Equipment Higher processing temperatures initiates grains formation Poor bonding of HAp film and metal surface 	[57–64]
Sputter coating	0.5–3 μm	<ul style="list-style-type: none"> Thick HAp coating layer Best for flat substrates Good bonding of HAp film and metal surface 	<ul style="list-style-type: none"> Lengthy coating process Expensive method Unable to process difficult shapes Amorphous coating layer 	[59,65]
High-velocity suspension flame spraying (HVSFS)	$\leq 50 \mu\text{m}$	<ul style="list-style-type: none"> Uniform coating layer Economical process No post treatment required Nanometric Porosity 	<ul style="list-style-type: none"> Requires higher temperatures 	[66–68]
Pulsed laser deposition	0.05–5 μm	<ul style="list-style-type: none"> Versatile method(dense or porous)/(Crystalline or amorphous) Uniform coating 	<ul style="list-style-type: none"> Costly process Pre-treatment of sample required Line of sight technique 	[69–71]
Hot iso-static pressing	0.2–2.0 mm	<ul style="list-style-type: none"> Uniformity of coating Processes all shapes(substrates) 	<ul style="list-style-type: none"> Expensive process Requires high temperature 	[72,73]
Flame spraying	100–250 μm	<ul style="list-style-type: none"> Most economical among all thermal spraying techniques Easily adaptable Porous coating 	<ul style="list-style-type: none"> Requires post treatment Crack develop at lower temperatures Microstructure consists of melted particles 	[74,75]

2. Theory of Adhesive Bond

The functionality and strength of coating layers on metallic substrate depend upon two fundamental characteristics i.e., cohesion and adhesion [76]. Adhesion is attractive force between various layers that hold the two surfaces. This force resists the applied stress to separate the two surfaces. Cohesion is the internal attractive force between molecules of a coating film. This force is responsible for holding the coating film bonded together as shown in Figure 1 below. The adhesion and cohesion forces between adhesive and metallic substrate are seen in Figure 1A,B respectively.



Figure 1. (A) adhesion and (B) cohesion forces between the adhesive layer and substrate [77].

The adhesive force between metallic substrate and adhesive is classified into three types (i) specific adhesion, (ii) mechanical force, and (iii) efficient adhesion [78,79]. The specific adhesion arises due to the presence of attractive forces between dissimilar molecules whereas mechanical adhesion is associated with forces present due to penetration of adhesive inside the microstructures of a substrate. At the same time, specific adhesion and mechanical adhesion combine to yield adhesion that holds the substrate and coating layer. The efficiency of this adhesion is dependent upon adhesive and cohesive forces. The adhesive layer failure results due to the breakage of the bond between the adhesive layer and substrate [80].

Theory behind Adhesion

Adhesives are non-metallic compounds used to bind two surfaces that hold them together and counter their separation. The application of adhesive offers several advantages, including stress distributions, ease in processing, aesthetic, and low processing costs. This adhesive penetrates down through micro-channels of a substrate and joins the two surfaces with strong binding force [81]. When different surfaces are bind with the help of adhesives, many other forces also act on these layers. These forces include physical adsorption, mechanical interlocking, and chemical forces. Adhesives are classified into two major classes named reactive and non-reactive adhesives. In the reactive class, the adhesive reacts with the surface molecules and forms a hard layer. The adhesive layer sticks to the surface of the substrate due to hydrogen bonding between substrate and adhesive. This transfer of hydrogen gives rise to electrostatic forces of attraction which are associated with the progression of Van der Waals forces between the molecules. The coating material and substrate are chemically interlinked with each other. The strength of these chemical bonds is very high, which resists the deterioration of coating against the external environment. The rough surface enhances the interfacial area for better contact between adhesive and substrate. To obtain maximum results from adhesive, the adhesive must possess wetting properties so that it can completely wet the surface. After application, it completely dries out and boosts its strength so that it shares and transmits the load between the adjacent layers [81–83].

3. Existing Challenges in Coating for Metallic Biomaterials

The adhesion of adhesive on the substrate will decide the surface and mechanical properties of metals used for biomedical applications. The improper coating on the substrate due to variation in process parameters increases the chances of sudden collapse when used as the bone supporting implants [84,85]. The poor coating layers will exfoliate and create serious effects during the tissue healing process. The coating pieces will leave the surface due to poor strength and affect the surrounding body parts [86,87]. The coating on metallic substrates is widely used to make it bio-compatible and bio-active. The crystalline nature of HAp offers better mechanical behavior against load and stress. Stability of HAp film is the biggest challenge in these coating implants. The complete degradation of the HAp occurred within the period of 4–5 years by natural cell mechanism with assistance of body environment like pH, water content and osteoclast cells. In vivo degradation of HAp can be started by dissolution or cell mediation. The speed of degradation also depends upon the chemical properties of HAp, Ca/P ratio, crystal size, crystallinity and porosity [88]. After this time, the malfunction (dissolution) can take place starting from the surface and penetrates down to the metallic substrate. Thus, stable HAp film will provide a reliable metallic implant for load-bearing applications. Operational difficulties during the

coating process also create problems for successful HAp coating with uniformity on metallic implants. The porosity and development of cracks on the coating surface is also an issue for the biomedical implant. Porosity is a very important parameter to judge the quality of ceramic coatings on biomedical implants. The porosity in coating layers dictates its bioactivity for biomedical implants. HAp offers more bioactivity and biocompatibility due to the presence of active agents calcium and phosphate which are in a similar ratio with human bone minerals [89,90]. Further enhancement of adhesive strength can be achieved by increasing the surface roughness and pores. For the further enhancement of bioactivity, the porous implants coated with HAp provide dual benefits. These implants have Young's Modulus closer to that of bone addressing the stress shielding effect and the increased surface area coated with Hap for good osseointegration [91,92]. A stress shielding effect arises when the modulus of the implant is greater than the young's modulus of bone. The support of the implant to the damaged bone is reduced as a result of this phenomenon. Due to this, the loads are taken up by the implant and shielded from going to the damaged bones [93]. According to Wolff's law, a bone developed its structure depending upon the force applied to it. The area of bone which experiences higher load will result in increasing bone density and vice versa. The decrease in bone mass results in the loosening of the implant [94]. Porous coating for bone regeneration allows the migration and proliferation of osteoblasts cells as well as vascularization. Additionally, the pores on the surface facilitate better mechanical interlocking between implant and bone. This interlocking provides higher mechanical stability which also reduces stress shielding [88]. Most pores are open and interconnected with each other. In vivo tests have shown that the pores facilitate cell migration, tissue growth, and transport of waste products [95].

4. Coating Methods

4.1. Sol-Gel and Dip Coating

Up till now, a lot of research work has been carried out using sol-gels and their application on metallic implants using the dip-coating technique. The coatings obtained by this technique possess the highest adhesion strength among all available technologies [42,96,97]. The success of the sol-gel method is due to the possibility of fabricating a wide range of materials, giving them a controlled porous microstructure [92]. The precursor mostly used for sol-gel preparation includes both calcium and phosphate-based salts. The universal solvent water and ethanol are commonly utilized for sol-gel synthesis [98–100]. Organic phosphorus compounds are dissolved in ethanol whereas in most of the cases, water is employed during sol synthesis [101,102]. The phosphorus solutions are mixed slowly with the calcium salt solutions drop wise [103,104]. Calcium nitrate salt is mostly utilized as a calcium source in HAp. Both solutions prepared separately are mixed and heated at various reaction temperatures. The sol-gel suspensions are prepared with the help of evaporation of excessive solvent present in the solution mixture. After evaporation of the solvent, the viscosity of the mixture increases to give a thick solution [105].

The apatite phase formation and nature of sol-gel are highly dependent on the type of salts used containing calcium and phosphorus and operating temperature. After evaporation, aging, drying and high-temperature calcination process are being applied to form sol-gel.

The sol-gel technique is well accepted and widely used due to its simplicity and cost-effectiveness. The superiority of this process over others is that it is capable to coat shapes with difficult geometrical symmetries. Additionally, it can offer greater coating strength along with higher adhesion [96,106,107]. The dip-coating technique is coupled with sol-gel to create a uniform coating layer on metallic bio-implants. Dip coating technique comprises of three-unit operations starting from (i) dipping step; (ii) removal step; (iii) drying period as shown in Figure 2.

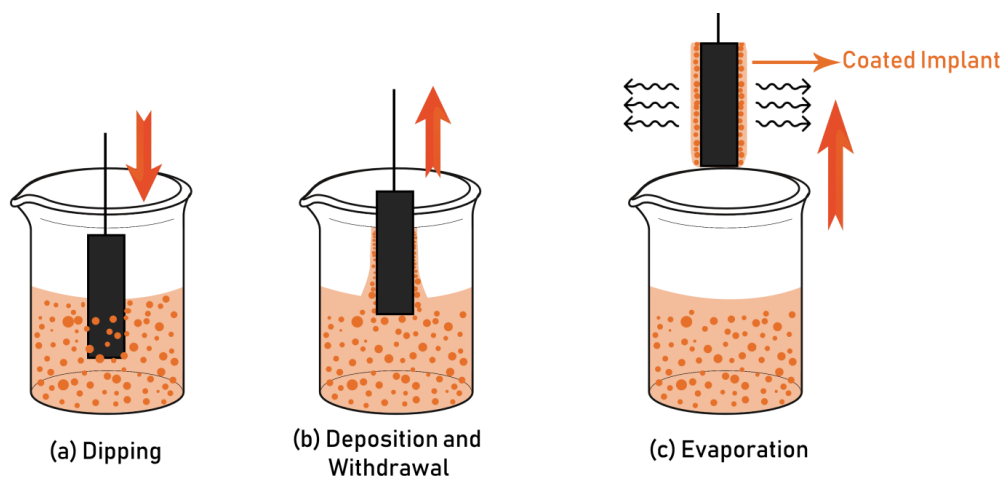


Figure 2. Schematic of Dip coating Process.

Dip coating possesses several characteristics including ease in processing, uniform coating layers, lower operating temperatures, cost-effective and process complex assemblies [108,109]. In this technique, the metallic substrate is immersed in the prepared HAp solution at a constant speed. After a fixed time interval of dipping the metallic substrate, pull out of the coating solution. The coating thickness is a function of speed, concentration of sol-gel, number of dips, and time of dipping. This method has good control over HAp film thickness [110,111]. HAp can be used single as well as with other polymers by making different blends. Several researchers used poly-(ϵ -caprolactone) (PCL) with a wide range of compositions ranging from 0–50 wt % with HAp. After preparation of coating solution, the metallic substrate is immersed in the HAp/PCL blend for 5 times at a rate of 200 mm/min [111]. Application of PCL promotes pore formation on the coating surface which enhances osseointegration that requires during the bone healing process. The research study shows that a 30/70 blend of PCL/HAp on Ti6Al4V metallic implant created a thick layer with even uniformity of 184 μm . On examination, the growth of cracks on the exterior layer of HAp were reduced which enhanced the adhesive force between metallic implant and HAp coating. The amount of cracks is directly linked with wear and corrosion resistance of metallic implant. Fewer the cracks greater will be the wear and corrosion resistance of implant. These cracks promote leaching of metals ions especially nickel and chromium into body thus cause harmful effects inside body including development of tumor and cancers [112–114]. After dip coating of synthesized HAp, heat treatment of coated implant is done for curing and to enhance its strength & density [113,115]. Heating of synthesized HAp at higher temperatures favored the removal of water content and promotes the formation of apatite structure within the coating layer. Various studies reported that the temperature of heat treatment ranging from 25–400 $^{\circ}\text{C}$ to maintain the surface textures and avoid the destruction of HAp structure [116–118]. Another research was carried out using 316 L stainless steel as an implant material. After application of <1 μm thick HAp coating, the material properties were enhanced. The annealing temperature of the coating ranged from 375–400 $^{\circ}\text{C}$ [36]. The coating on the implant possesses a bonding strength of 44 MPa upon testing. Further enhancement of adhesive strength can be achieved by increasing the surface roughness and pores. The combined arrangements of sol-gel and dip coating techniques are extensively used due to their simplicity, compatibility, and low cost to prepare bio-compatible implants. By comparing factors including coating time and shapes limitations is less for dip coating. Coating time is very less while dip coating can process irregular geometries. Another major advantage of this process is its mild operating conditions during coating. Moreover, sol gel and dip coating techniques yield uniform & thick HAp layer and better Ca/P ratio (1.67–1.76) in comparison to all available processes. Table 3 shows different raw materials and operating parameters used for the synthesis of sol-gels.

Table 3. Literature related to Sol-gel HAp Coating.

Sr.No	Precursor for Sols and Other Materials	Solvent	Implant Metal	Operating Conditions	Outcome	Year	References
1	Triethylphosphite and calcium nitrate	Water	Stainless steel 316 L	<ul style="list-style-type: none"> Drying of coating at 80 °C for 15 min Annealed at 375 °C, 400 °C, and 500 °C in air Dipping speed 5 cm/min. 	<ul style="list-style-type: none"> Annealing at 500 °C for 15 min leads to development of nano crystals and micro-cracks. Nano-cracks behave like natural bio-crystals 	2002	[36]
2	Titanium propoxide, Di-ethanolamine, Calcium nitrate, tetrahydrate and Triethylphosphite	Water and ethanol	Titanium	<ul style="list-style-type: none"> Temperatures of 400–500 °C. Thicknesses of 800 and 200 nm. 	<ul style="list-style-type: none"> Enhancement of bioactivity and osteoconductivity of Ti Implant 	2004	[119]
3	Calcium nitrate tetra-hydrate, Tri-ammonium phosphate tri-hydrate and Gelatine	Water	Titanium	<ul style="list-style-type: none"> Reaction at room temperature pH 6.0–7.8. Annealed at 460–750 °C in argon media 	<ul style="list-style-type: none"> Bioactivity increases after application of coating 	2005	[37]
4	Calcium Nitrate, Strontium Nitrate and Phosphorus penta oxide	Ethanol	Titanium	<ul style="list-style-type: none"> Dipping Speed of 8 cm/min. 15 min drying at 150 °C 15 min firing at 700 °C 	<ul style="list-style-type: none"> 10% SrHAp coating yields enhanced osseointegration compared to HA. The bone area ratio and bone-to-implant contact increased by 70.9% and 49.9% 	2010	[41]
5	Triethylphosphite and Calcium nitrate	Water, Acetone, Ethanol	Nickel-Titanium Alloy	<ul style="list-style-type: none"> Dipping time rinsed 5 min Withdrawn speed of 20 mm/min Drying at 80 °C Annealing in air at 450 °C for 2 h. 	<ul style="list-style-type: none"> Rate of Ni ion release decreases through the Hap coatings 	2011	[42]
6	Calcium nitrate Tetra hydrate, phosphorous penta oxide	Ethanol	Magnesium AZ91	<ul style="list-style-type: none"> Reaction Temperature at 26 °C for 5 h Withdrawn speed 0.1 mm/s Drying at 60 °C for 24 h Calcination and sintering at 400 °C for 6 h 	<ul style="list-style-type: none"> HAp coating stabilizes alkalization behavior Improved corrosion resistance 	2013	[44]
7	HAp Nano-particle	-	Titanium	<ul style="list-style-type: none"> Heat treatment at 550 °C for 5 min in air Nanoparticle stabilization at pH = 9 	<ul style="list-style-type: none"> Nano HAp coating has higher impact on earlier healing periods Micro structures are more influential at completely healed stages 	2013	[43]
8	Titanium isopropoxide, Calcium acetate monohydrate, 1,2-ethandiol, poly vinyl alcohol, Triethanol amine and ortho phosphoric acid	Water	Titanium	<ul style="list-style-type: none"> Reaction temperature 65 °C Initial heat treatment at 650 °C for 5 h Coated samples annealing at 650 °C for 5 h 	<ul style="list-style-type: none"> Increasing HAp layers enhances hydrophilicity Initial heat treatment enhances HAp layer adhesion 	2016	[120]

4.2. Biomimetic Deposition

The biomimetic method constitutes of mimicking natural building processes of bone. In this way, HAp can be used to enhance the osseointegration of natural bone and coated artificial implant [121,122]. The biomimetic coating process promotes the adhesion and proliferation of osteoblast cells, as it mimics the properties of natural bone tissues. A biomimetic method like other chemical coating processes needs the presence of hydroxyl groups on the surface of the implant. This functional group can easily attach with the pre-treatment step using acid or alkali. These functional groups on the substrate surface facilitated the CaP nucleation process with succeeding crystallization to promote apatite formation. The biomimetic coating processes occurred at normal conditions of pH and temperature [123–126]. Figure 3 below shows a biomimetic coating in SBF. Table 4 shows different raw materials and operating parameters used during the biomimetic coating.

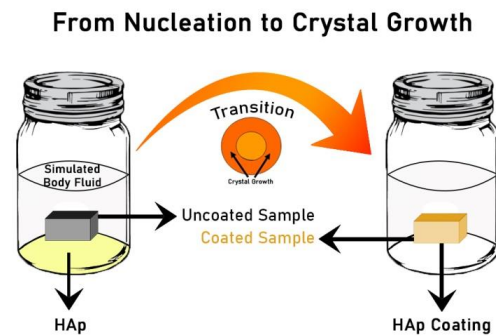


Figure 3. Biomimetic coating using HAp in Simulated body fluid (SBF).

Table 4. Raw materials and operating parameters for biomimetic coating.

Sr.No	Coating Material	Solvent	Implant Metal	Operating Conditions	Outcome	Year	References
1	Calcium phosphate, Tobramycin	Water	Titanium alloy	<ul style="list-style-type: none"> • 37 °C • 24 h • pH 5 or 7.3 	<ul style="list-style-type: none"> • Coating containing antibiotics prevent post-surgical infections. 	2002	[124]
2	Calcium phosphate	Water, Human blood plasma (HBP), Simulated body fluid (SBF)	Titanium and tantalum	<ul style="list-style-type: none"> • Temperature 37 °C • 24 h • Stirring rate 250 rpm • pH 7.1 	<ul style="list-style-type: none"> • Biomimetic coating facilitated rapid bone formation around the implant • Reducing recovery time after surgery. 	2004	[127]
3	Calcium phosphate, CaO–SiO ₂ based glass	Water, Simulated body fluid (SBF)	Titanium	<ul style="list-style-type: none"> • Method-1 the metallic sample was placed on glass particles and soaked in SBF at 37 °C in a glass container for 6 days. The sample was immersed thereafter in SBF for 10 days • In method-2, the sample was directly immersed in SBF solution at 37 °C and examined up to 13 days. 	<ul style="list-style-type: none"> • Thickness of coating was found to increase with the increase in immersion time. • The use of glass did not help the formation of apatite • The coating obtained by this method was also not uniform. 	2005	[125]
4	Sodium hydroxide, Calcium phosphate,	Water	Titanium	<ul style="list-style-type: none"> • Surface activation in 10 M NaOH • Room temperature • Voltage of 10 V • Time 30 min. • pH > 7 	<ul style="list-style-type: none"> • Coating thickness 50 μm was achieved • Coating promote bone in growth 	2008	[128]
5	Hydroxyapatite and tri-calcium phosphate	Water	Titanium alloy	<ul style="list-style-type: none"> • Mix the solution well for 2 h • Stirring speed 700 rpm • Temperature 37 °C 	<ul style="list-style-type: none"> • An adequate and uniform hydroxyapatite coating on pure titanium substrates in a shorter period of time • Coating promotes osseointegration. 	2015	[129]

4.3. Chemical Vapor Deposition

Chemical vapor deposition (CVD) is a coating technique that uses volatile precursors to coat pre-heated substrates via reaction or decomposition on the surface as shown in the Figure 4 [130,131]. CVD is widely used to coat metal implants with HAp and calcium phosphate-based coating [132]. The most promising feature of CVD is that it can control the crystal phases and micro-structures formation during coating. Additionally, it can able to coat complex metallic shapes with uniform coating [131]. Table 5 below shows different raw materials and operating parameters applied during CVD.

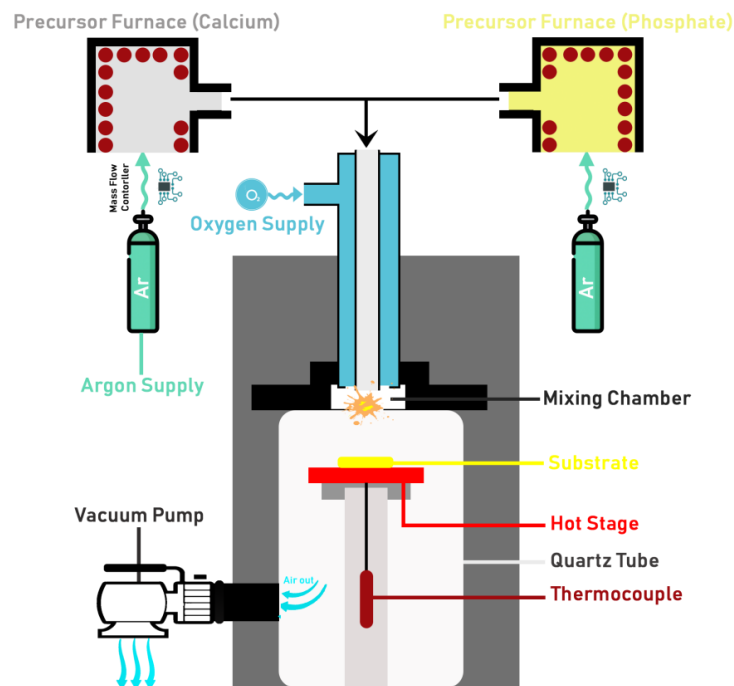


Figure 4. Schematic of HAp coating using Chemical Vapor Deposition (CVD).

Table 5. Material and operating parameters for CVD.

Sr.No	Precursor	Carrier Gas	Implant Metal	Operating Conditions	Outcome	Year	References
1	Calcium diketonate and tri-methyl phosphate	Oxygen	Titanium	<ul style="list-style-type: none"> • Temperatures from 500 °C to 650 °C • Pressure 10 Torr • Growth rate 15 nm/min • Thickness range from 0.1–1 micrometer 	<ul style="list-style-type: none"> • HAp coatings with Ca/P ratio of ~1.67 were amorphous. • Coatings with Ca/P ratio of 1.5 ± 0.5 and 1.0 ± 0.5 were crystalline. • Coatings were very dense and free of cracks. 	1998	[133]
2	Fluorine-containing carbonated hydroxyapatite, 2,2,6,6-tetramethylheptane-3,5-dione	Argon	Titanium	<ul style="list-style-type: none"> • Substrate temperature 600 °C • Post heat treatment in air at 800 °C for 3 h 	<ul style="list-style-type: none"> • The coating has a cauliflower-like agglomerated structure and composition with some similarities to human bone mineral 	2004	[134]
3	Calcium dipivaloylmethanate and Titanium di(i-propoxy)bis (dipivaloylmethanate)	Argon	Titanium	<ul style="list-style-type: none"> • Pressure 0.8 kPa • Deposition temperature 873–1073 K • Deposition time 0.3–0.9 ks 	<ul style="list-style-type: none"> • The coating was affected by substrate temperature 	2007	[135]
4	Bis-dipivaloylmethanocalcium and Triphenyl Phosphate	Argon	Titanium	<ul style="list-style-type: none"> • Pressure 800 Pa • Deposition temperature 973 K 	<ul style="list-style-type: none"> • HAp-coated excellent mechanical biocompatibility 	2010	[136]

4.4. Electro-Chemical Deposition

The most commercially adopted coating technique is Electro-chemical deposition for biomaterials [113]. Electro-chemical deposition uses charges associated with two-electrode systems i.e., anode and cathode as shown in Figure 5. The effectiveness of this process is the combination of both anodic and cathodic coating. A single coating layer by anodic deposition is unable to meet the requirement of small-sized structures on the surface of metallic implant. To minimize the defects cathodic deposition is mostly applied on a commercial scale for coating bio-implants [137,138]. Two operational methods come under the umbrella of electro-chemical deposition, i.e., (1) the electrophoretic procedure (EPD), and (2) the electrolytic procedure (ELD). EPD uses suspended ceramic particles whereas ELD utilizes metallic salts from saturated salts solution. Titanium implants are mostly employed in coating process using ELD or EPD techniques [139,140]. Applied voltage and deposition time are important factors in this type of coating [141]. The process starts after HAP precursor salts are dissolved in water which acts as an electrolyte [142,143]. One of the salient features of this method is the capacity to produce thick uniform coating along with high production rates [144–146]. Lower operating temperature is mostly used during process whereas energy consumptions are normally on higher side due to involvement of electricity. Many researchers worked on the electro-chemical deposition of HAP on metal implants as tabulated in Table 6. By this technique, a homogenized layer of HAP formed on the metal surface with higher force of adhesion.

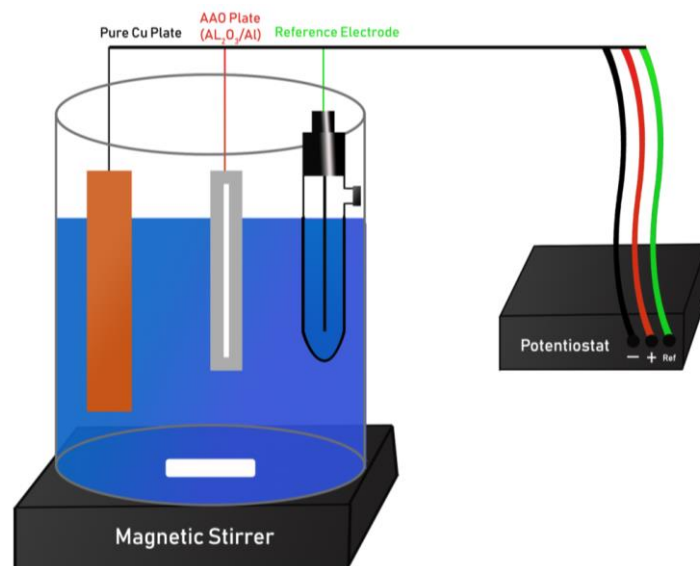


Figure 5. Schematic of Electro-chemical deposition Process.

Table 6. Research Studies related to Electro-Chemical Deposition.

Sr.No	Electrolyte and Other Chemicals	Solvent	Implant Metal	Operating Conditions	Outcome	Year	References
1	Calcium nitrate, Ammonium di hydrogen phosphate, Sodiumnitrate, Hydrogen peroxide, Zirconium oxide	Water, Ammonia, Nitric acid	Nickel -Titanium	<ul style="list-style-type: none"> pH 6.0 at 25 °C NiTi as the anode and graphite plate as the cathode. Current density at 0.5 mA/cm² for 40 min Temperature at 65 °C. Drying at room temperature in air 	<ul style="list-style-type: none"> Zirconia enhances bonding strength between coating and substrate. Corrosion resistance of NiTi increased 60 times after coating in body fluid at 37 °C. 	2010	[50]

Table 6. Cont.

Sr.No	Electrolyte and Other Chemicals	Solvent	Implant Metal	Operating Conditions	Outcome	Year	References
2	Calcium nitrate and Sodium hydrogen phosphate and Tris-hydroxy-methyl-amino-methane	De-ionized water	Cobalt -Chromium -Molybdenum	<ul style="list-style-type: none"> 200 nm thickness CoCrMo as the cathode and platinum as the anode pH at 6 Electrolyte stirring at 250 rpm Drying of coating at room temperature 	<ul style="list-style-type: none"> Strong mechanical bonding strength to the substrate as compared to other techniques. 	2011	[51]
3	Calcium chloride, Ammonium di hydrogen phosphate, Sodium hydroxide	Distilled water	Titanium	<ul style="list-style-type: none"> pH at 6.0 Temperature at 80 °C for 30 min Ti as cathode, Pt as anode and Ag/AgCl as reference electrode 	<ul style="list-style-type: none"> The coated implant was bioactive when in contact with SBF 	2012	[147]
4	Calcium nitrate, Ammonium di hydrogen phosphate, Titanium nano tubes	Distilled water	Titanium	<ul style="list-style-type: none"> pH of electrolyte at 7.2 Titanium as cathode and Platinum as an anode Electro-deposition of HAp at potential, -2.5 V for 10 min Temperature 80 °C 	<ul style="list-style-type: none"> TiO₂ nano-tubes improved adhesion of HAp Bones tissue growth also increases 	2014	[148]
5	Calcium nitrate, Ammonium di hydrogen phosphate	Distilled water	Magnesium	<ul style="list-style-type: none"> Applied voltages were 90, 100, 110 and 120 V. Time intervals 20, 30, 40 and 60 min Temperature 80 °C. Drying in autoclave at 140 °C for 4 h 	<ul style="list-style-type: none"> Corrosion resistance increases after coating of HAp HAp enhances bioactivity in SBF 	2015	[149]
6	Calcium nitrate, Ammonium di hydrogen phosphate	Distilled water	Ti6Al4V Alloy	<ul style="list-style-type: none"> Cathode was Ti6Al4V and anode was a platinum plate Temperature 90 °C Deposition time 60 min g Current densities were 1.25, 1.87, 2.50, 3.12 and 3.61 mA/cm². 	<ul style="list-style-type: none"> HAp coating increase bioactivity. 	2016	[142]
7	Calcium nitrate, Ammonium di hydrogen phosphate	Ultra purewater	Pure titanium	<ul style="list-style-type: none"> Cathode was titanium and platinum was anode pH maintained at 5 Coating temperatures 50 °C and 75 °C Drying at room temperature in a desiccator. 	<ul style="list-style-type: none"> Higher temperature favored thick coating with superior wet ability 	2018	[150]

The researchers recently used reinforced material along with HAp to increase the mechanical properties of metallic biomaterials. These reinforced substances including zirconia oxide (ZrO₂), carbon nanotubes (CNTs), and titanium oxide (TiO₂) [53,151–154]. The block diagram of electro-chemical deposition process is shown in Figure 6. HAp nanoparticles coating also applied which yielded better results as compared to pure HAp coating. The strength of HAp coating was enhanced in a research by adding single walled nano tubes (SWNT). This blend increased the coating homogeneity along with its crystallinity. The coating on metallic implant showed a defect free surface with no cracks. Furthermore, the bond strength between HAp coating and metallic implant increases from 15.3 to 25.7 MPa after blending of SWNTs [155]. HAp coatings formed using electro-chemical methods were more compact and uniform due to phenomena of nucleation and growth behind the deposition. Also the coating enhanced cell attachment and proliferation on the samples thus making it an ideal candidate for orthopedic implants [156]. Process and annealing temperatures were the critical factors deciding the nature of the coating. Chemical assisted heat treatment after electrochemical deposition

increased coating density, adhesion, and bond strength [157]. Thus, electro-chemical deposition method showed a lot of potential for future bio-medical applications.

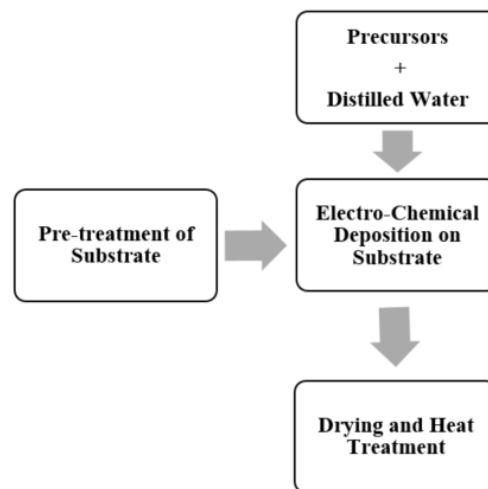


Figure 6. Block Diagram of Electro-Chemical Deposition Process.

4.5. Thermal Spraying

The thermal spray technique is gaining a lot of attention and adopted as a latest method of coating which gives excellent properties to bio-medical metallic implants. In thermal spray, precursors in the form of solution or suspension are used for coating the desired substrate to impart desired properties. Thermal spraying is classified into three sub-groups, namely flame, plasma arc, and electrical arc sprays. There are different operational approaches to carry out thermal spraying on substrates. These approaches include atmospheric plasma spraying (APS), vacuum plasma spraying (VPS), liquid plasma spraying (LPS), suspension plasma spraying (SPS), high-velocity oxy-fuel (HVOF), high-velocity suspension flame spraying (HVSFS), detonation gun spraying, and gas tunnel type plasma spraying (GTPS). All these techniques were used to coat metallic implants with HAp [158–163].

4.5.1. Plasma Spraying

Plasma spray is a commonly used technique nowadays to coat bio-active HAp on bio-medical implants [164–166]. This technique used an electric arc of high temperature and pressure for melting and showering of HAp on the metallic implants. The starting material of coating is dried HAp which is converted into plasma with the help of thermal plasma jet. After that the generated high temperature plasma contacts the surface of substrate and adheres on it as shown in Figure 7. Another type of plasma deposition includes air or vacuum spray, which is a more established technique. The HAp coating on a substrate by using this technique is stronger with superior properties. The temperature of jets varies from 10,000 K–30,000 K which decreases with a decrease in distance from the jet nozzle [167,168]. This particular technique is used for bio-active coatings on different bio-medical implant materials. The only limitation of the plasma spray process is the deformation of HAp structure due to high temperature coating operation. Sometimes high temperature operation causes reduced adhesive strength of HAp layer and metal surface [169]. The structural properties of coated HAp can be altered by using post heat treatment. The coated HAp annealed at 400 °C for 90 h. This results in the transformation of HAp structure and increased its crystallinity [170]. Higher crystalline structure favors good adhesive strength between implant and damaged tissues [171]. On the other hand, high temperature heat treatment also reduces the fatigue stresses on the surface as coating thickness decreases along with the color of coating. This post coating heat treatment at 700 °C for 1 h also enhances the purity of coating by removal of any excess water and impurities [172,173]. The metallic implants coated with HAp using plasma spray enhance the osteoconductivity due to the strong bonding

of HAp with the metal surface [174–176]. The research studies using the plasma spray technique are displayed in Table 7 below.

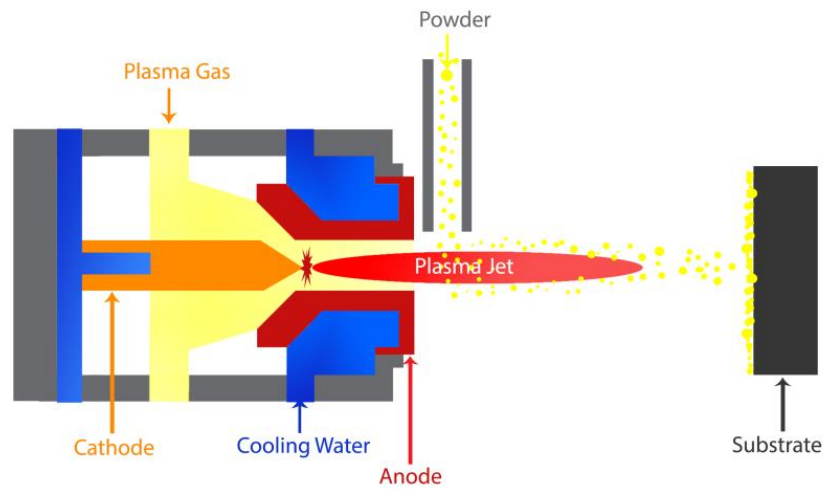


Figure 7. Plasma Spray Coating.

Table 7. Literature related to Plasma Spraying Using HAp.

Sr.No	Raw Materials	Metallic Implant	Process Conditions	Outcome	Year	References
1	HAp, Al ₂ O ₃	Titanium	<ul style="list-style-type: none"> Hap particle size 45 μm. Current 450–750 A Gas flow rate 33–61.4 Scfh Powder flow rate 10–20 g/min Spray distance 80–120 mm Carrier gas flow rate 4.7–9.4 Scfh 	<ul style="list-style-type: none"> Highest coating crystallinity results at high current, low spray distance and low carrier gas flow rate. 	2015	[168]
2	HAp, Al ₂ O ₃	Titanium	<ul style="list-style-type: none"> Traverse speed 38 mm/s Spray time 35 s Spray gun passes 15 	<ul style="list-style-type: none"> Osteogenic response enhances after application of bio-active coating. 	2017	[169]
3	HAp, Al ₂ O ₃ , Tri-Calcium Phosphate	Steel	<ul style="list-style-type: none"> Torch speed 50, 200, and 500 mm/s Primary plasma gas (Ar) flow rate 45 Slpm Secondary plasma gas (H) flow rate 5 Slpm Arc current 530 A Standoff distance 85mm Suspension pressure 1 bar Suspension feed rate 25 g/min 	<ul style="list-style-type: none"> Hap coating thickness 28 μm. Coatings were porous with pore size 0.2 to 6 μm 	2018	[166]

4.5.2. High-Velocity Suspension Flame Spraying (HVSFS)

A high-velocity oxygen-fuel flame spray technique has been used to obtain uniformity by coating suspensions using a spray mechanism as shown in Figure 8 [177,178]. Few difficulties may encounter due to the handling of suspensions. This problem can be resolved by using axial powder injection. In this process, high-velocity suspension flame spray (HVSFS) covers the injection complications [68,179]. The coatings obtained are very dense and uniform with this technique. The salient features of this process include lower cost with high efficiency along with no post-treatment requirements [180,181]. The HVSFS process yields better coatings with uniform structure when the desired thickness is less than 50 μm [182]. The coating properties, especially the ones involving bonding strength between the substrate and coated layer produces from HVSFS techniques tend to be affected seriously due to the effect of processing parameters such as gas flow, air-fuel ratio spray distance, and electric arc current, as tabulated in Table 8. The higher thickness of coating tends to decrease the mechanical properties along with adhesive bonding of coating with the metal surface. Stresses also started to generate on the metallic surface due to the thick coating. Due to poor bonding, the coating starts to disintegrate and

exposes the metallic surface to the body fluid. This results in the discharge of metallic ions as a result of corrosion of the metallic surface after dissolution of the protective oxide film [183].

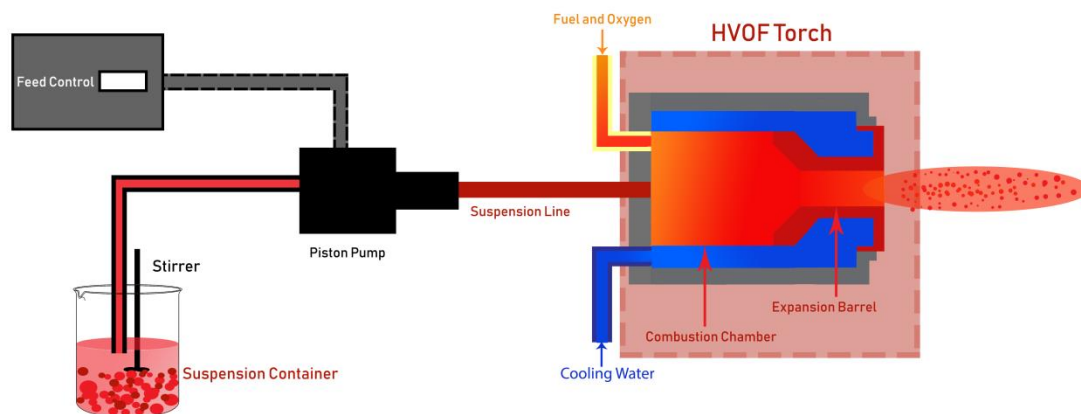


Figure 8. High velocity suspension flame spray (HVSFS).

Table 8. Recent Studies on HAp coatings Using HVSFS.

Sr.No	Coating Materials	Metallic Implant	Solvent	Process Conditions	Outcome	Year	References
1	HAp	Titanium	Water or Di-ethylene glycol (DEG)	<ul style="list-style-type: none"> Low surface temperature 350 °C for Water Suspensions High surface temperature for DEG suspensions 550–600 °C 	<ul style="list-style-type: none"> DEG coatings are more stable in SBF solutions than water suspension coatings DEG coatings are more crystalline and reliable. 	2011	[158]
2	HAp	-	Water or Di-ethylene glycol	<ul style="list-style-type: none"> Temperature Range 357–616 °C Torch Cycle 2–4 	<ul style="list-style-type: none"> HAp coatings using HVSFS are dense and more reactive than SPS due to higher calcium phosphate content. 	2015	[68]
3	HAp/TiO ₂	316 L Stainless Steel	Water and Iso-propanol	<ul style="list-style-type: none"> Pre-heating of substrate 150–200 °C Spray distance 100 mm Compressed air for cooling 	<ul style="list-style-type: none"> Tensile strength and wear resistance of HAp/TiO₂ double-layer coatings are enhanced as compared to single HAp coating. 	2018	[184]

4.5.3. Pulsed Laser Deposition

Pulsed laser deposition (PLD) is a coating technology used to coat different substrates with the help of a highly accelerated beam of laser in the presence of a vacuum as shown in Figure 9. This laser beam strikes the targeted substrate with the material which we want to coat. The coating material starts to vaporize and form high-temperature plasma. This plasma strikes the target material and forms a thin layer of coating. For better coating and thin film without any defects, high vacuum atmosphere is favored. Heating of the substrate is also favored for achieving uniformity in coating [185]. PLD process has gained much attraction due to versatile coating characteristics along with a wide range of operational parameters as shown in Table 9. These parameters include uniformity, thickness, strength, crystallinity etc. [186]. The drawback of this process includes residual stresses which are associated with the failure of the coating. These residual stresses arise due to high temperature operation [187]. Another reason behind residual stresses is difference in crystal structure of HAp coating and metallic substrate. These residual stresses create defects on coating films which are unable to detect on a very thick layer (1 μm thickness). Surface roughness also plays an important role during bone healing. The coating formed during PLD is more uniform which affects the response of nearby bone tissues for tissue regeneration. The coatings formed by PLD are mostly uniform with slight micro porous structure with surface roughness ranges up to a few nanometers [188]. For minimizing

the stresses, post heat treatment operation is usually carried out. For the bio-implant, the existence of surface irregularities and porosity promote cell adhesion and proliferation due to larger surface area [189]. The response of the body towards HAp coating is affected by the particle size, texture, morphologies and surface area provided [190]. The rough surfaces of coating enhance the wettability which is required during growth and interaction with body fluids [190]. Coating surface chemistry and topography are also vital for good osseointegration [191]. The healing of damaged bone in the presence of a biomedical implant is similar to primary bone healing. At starting, blood is present which gradually transformed in to clot in between the implant and bone. This transformation is completed in the presence of phagocytic cells. If the implant is already coated with the bioactive coatings the response generated by them is fast. This response facilitated in quick bone regeneration in comparison with metallic implants without coatings. The bioactive coatings promote biological responses from the body e.g., bonding with tissues and tissue growth. Normally, there are two types of materials available. One possesses the property of osteoconductivity whereas the other offers osteoproductivity. Once these coating layers interacted with the body fluid they started to generate stimulus which facilitates in the bone growth process along the surface or away from the biomedical implant [192].

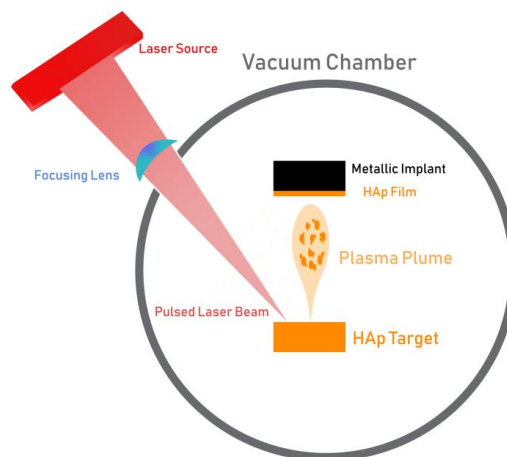


Figure 9. HAp coating using Pulsed Laser Deposition.

Table 9. Literature related to Pulsed Laser Deposition.

Sr.No	Coatings	Metallic Implant	Process Parameters	Outcomes	Year	References
1	HAp	Titanium	<ul style="list-style-type: none"> Post treatment at 550 °C for 1 h Vacuum Atmosphere Substrate at room temperature 	<ul style="list-style-type: none"> Thickness 1 μm The mechanical properties are less as compared to sputtered ones. 	2004	[193]
2	HAp	Silicon(100) and Titanium	<ul style="list-style-type: none"> Room Temperature Annealed 500 °C 	<ul style="list-style-type: none"> Crystalline coating Heat treatment after coating enhances mechanical properties 	2005	[194]
3	HAp	Titanium	<ul style="list-style-type: none"> Ambient Temperature Pressure 10⁻⁴ to 10⁻¹ torr of oxygen Annealing at 290–310 °C in air. 	<ul style="list-style-type: none"> Purity increased after post treatment Crystalline HAp coatings showed no dissolution in SBF. 	2009	[117]
4	HAp	Titanium	<ul style="list-style-type: none"> UV KrF laser $\lambda = 248 \text{ nm}$ and $\tau = 25 \text{ ns}$ Post treatment at 400 °C for 6 h in water vapors 	<ul style="list-style-type: none"> Film Thickness ranging 100 nm to 1 μm 	2011	[195]
5	HAp and Silicon	Titanium	<ul style="list-style-type: none"> Pulse repetition rate 5 Hz Temperature of substrate 400 °C, 500 °C, and 750 °C $\lambda = 248 \text{ nm}$ and $\tau = 17 \text{ ns}$ 	<ul style="list-style-type: none"> Coatings were dense, crystalline, and nanostructured, which enhanced hardness The bioactive Si-HAp coatings improved the osseointegration. 	2014	[196]

4.5.4. Flame Spray Coating

Flame spraying (FS) technique was the first-ever thermal spray method developed in the year 1910. FS is the most economical and easy technique among all the thermal spray coating methods [197]. Flame spray coating started by the combustion of oxygen flame for melting the HAp powder which yields porous and composite coating on metallic surfaces as shown in Figure 10. FS possesses a lot of disadvantages in comparison to other thermal spray coating techniques. These disadvantages include a bigger size of microstructure, pore size, and cracks on the coating layer. As mentioned earlier, FS is economical with ease of operation in terms of commercial processes. The particle velocity for the process ranges from 200–300 m/s with new modernized torches. An oxygen and acetylene blend is used as a fuel to power the torch to achieve higher combustion temperatures around 2600 °C [198–201]. The flame spray method was used to deposit zinc-doped HAp on Ti-6Al-4V substrates to enhance its biocompatibility and antibacterial activity against *E. coli* [199]. Liu and coworkers deposited porous HAp coating on titanium implant using flame spraying. Wetting of metallic substrate before coating generates porous coating. The wetting method enhances the cell proliferation and differentiation of pre-osteoblast cells. The coatings developed under wet conditions contain many cracks and fissures in the range of nano-size ~100 nm [197]. Monsalve and co-workers [75] coated 316 L steel and titanium alloys with bioactive glass coating using the flame spray technique. The magnesium content present in the bioactive glass affects the crystallinity of the coating layer. The higher content favors a more crystalline coating layer that favors pores formation. Additionally, the lower thermal conductivity of titanium alloys promotes higher crystallinity in accordance with slow cooling rate. This helps to form some crystalline phases. When the coated substrate is immersed in the SBF solution, hydroxy carbonate apatite layer is formed, which confirmed its bioactivity.

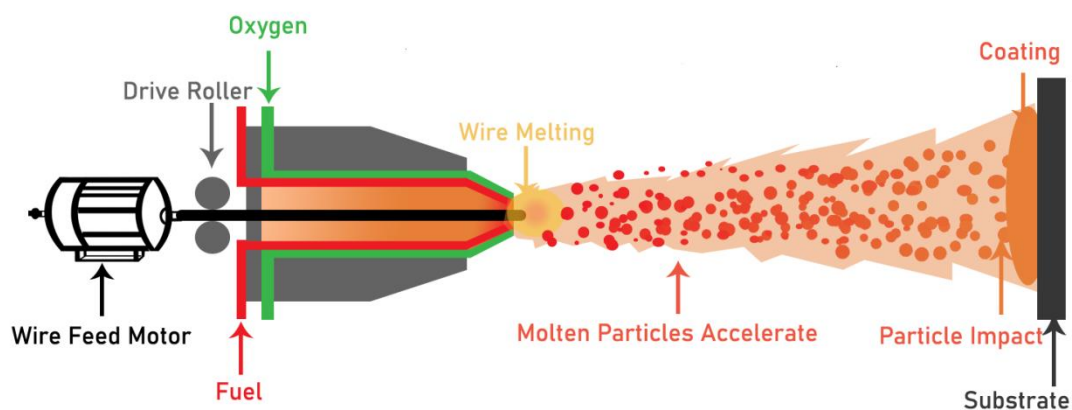


Figure 10. HAp coating using Flame Spray Technique.

5. Innovative Methods of Coating

Yuan and Golden used HAp to coat stainless steel (SS) 316 L with electro-deposition [202]. The substrates were coated with two layers to minimize the contact of the implant with body fluid. After the coating process, heat treatment was employed to samples in a vacuum at 800 °C or in presence of air at 600 °C. The benefit of bi-layer coating was to enhance uniformity with high bonding between surface and HAp along with bioactivity. Another innovative method includes the introduction of an oxide layer in between metallic implant and HAp as shown in the Figure 11. This oxide film protects the metallic surface and prevents the release of toxic ions from the top metallic layer [54,203,204]. The oxide layers covered with HAp coatings enhance the adhesion of oxide and HAp [205,206]. The metallic coating also reduces the cytotoxic effects and enhances the biological performance of the implant [206,207]. Ceramic material like Zr was also applied in between the HAp and metallic surface. This ceramic layer acted as a strong bond and worked as a composite. This type of coating was favorable for implants subjected to cyclic stresses [208]. The bond strength enhancement between metallic

implant and coating is a very important factor for the reliability of the implant. The super-high-speed (SHS) blasting method is a new and novel technique that not only enhances the bond strength but also eliminates exfoliation of HAp layers. The HAp film obtained from the SHS method yields higher adhesion strength and outstanding wettability properties [209].



Figure 11. (A) Oxide layer in between metallic implant and HAp and (B) Bi-layer Metallic oxide coating.

Another innovative technique was the combination of two coating method to produce HAp films performed by Jia et al. [210]. The researchers coupled micro arc and sol-gel processes together to form coating layers. The micro-arc improved the biocompatibility of the metallic implant, and the bioactivity was enhanced further by the sol-gel HAp coating on the anodized Ti [211].

6. Conclusions and Future Perspective

The main target of this review is to gather a broad literature bank associated with the hydroxyapatite coatings and coating methodologies for the development of biomedical implants.

HAp coatings especially nanocrystals of HAp enhance the biocompatibility of biomedical implants more which mimic the implant like natural bone. The four most commonly applied methods were discussed here with their parameters and efficiency. Thermal spray coatings are most efficient and commonly applied on metallic implants due to their uniform coating layer on the metal surfaces, in recent years. High temperature and high speed of jets permit the HAp particles to deposit the surface with the elimination of defects due to higher melting points of ceramic materials.

The coating thickness can be varied up to several microns with some carbide formation which provides porous surface and strength to coating. Sol-gel method is able to process a wide range of HAp pre-cursors in aqueous form for coating with any shape of the implant. Electro-chemical deposition also utilizes raw materials in aqueous form for coating on biomedical implant assisted by potential difference of electrochemical cell. A wide range of concentrations can be used for coating on complex shapes. The only drawback of this method is the poor conductivity of substrates which creates a hurdle in the free movement of charges. Innovative methods are also discussed here which increase the performance of implants even more in the body. Intermediate oxide layers between the metallic surface and HAp enhances the adhesion of HAp. Pre-treatments and post-treatment of HAp coating and implant surface increase the implant efficiency and makes the biomaterial more feasible for placement in the body.

Although it has been decades working and exploring HAp and its applications in biomedicine, yet there are important areas that have either not been explored well or are very rarely tested in vivo. For example, as described earlier, the adhesion strength of the HAp coating is a critical factor. Therefore, developing a coating of nanoparticles on titanium alloy implants can increase the surface area of the implant. This nanoparticle-coated titanium alloy can further be coated with HAp crystals for increased biocompatibility. The increased surface area will ultimately provide a better adhesion strength to coating keeping the biocompatibility and bioactivity factor intact. Along with this, the use of porous titanium alloys coated with HAp has also not been investigated well. These porous implants coated with HAp give dual benefits. These implants have Young's modulus closer to that of bone addressing the stress shielding effect and the increased surface area coated with HAp providing biocompatibility along with osseointegration.

Another important area that needs to be explored is the use of HAp in combination with other calcium magnesium phosphates naturally present in bones. These other phases have important functions during bone tissue healing. Whitlockite is one of the calcium magnesium phosphate that is naturally present in bone and plays an important role because of its osteogenesis properties [212,213]. Synthesis of whitlockite is a very critical process and requires extensive optimization of parameters like pH and temperature. It can therefore be the reason for not exploring the coating involving different other phases, particularly whitlockite that has not been investigated comprehensively. Following this, HAp in combination with different ions substituted whitlockite can also provide better osteogenic properties. A study has been already performed using a combination of HAp, whitlockite and chitosan which was concluded with very positive tissue healing results [214] but this along with other combinations need to explore comprehensively both in vitro and in vivo. Thus, the use of HAp coating on nanoparticle-coated titanium implants, both bulk and porous, and the use of biphasic coatings, particularly combining HAp with other available calcium magnesium phosphates, is prospective options in this area for the future.

Author Contributions: Conceptualization, B.B. and U.L.; Writing—original draft preparation, B.B., M.F.K.N., I.D., and U.L. writing—review and editing, B.B., U.L., M.Z., and M.B.K.N.; supervision, U.L. All authors have read and agreed to the published version of the manuscript.

Funding: The APC was partially funded by National University of Sciences and Technology, Islamabad. There was no external funding.

Acknowledgments: This work was conducted at the School of Chemical and Materials Engineering (SCME), National University of Sciences and Technology, Sector H-12, Islamabad. U.L. acknowledges the financial and administrative support from the SCME, NUST.

Conflicts of Interest: The authors declare no conflict of interest.

Nomenclature

Symbols

HAp	Hydroxyapatite
FDA	The food and drug administration (USA)
RF	Radiofrequency
MAO	Micro-arc oxidation
CVD	Chemical vapor deposition
PLD	Pulsed laser deposition
HVSFS	High-velocity suspension flame spraying
PCL	Poly-(ϵ -caprolactone)
EPD	Electro-phoretic deposition
ELD	Electrolytic deposition
SBF	Simulated body fluid
FS	Flame spraying
SWNT	Single-walled nano-tubes
SLPM	Standard liters per minute
SCFH	Standard cubic feet per hour
SHS	Super-high-speed

References

1. Nasab, M.B.; Hassan, M.R.; Sahari, B. Metallic biomaterials of knee and hip: A review. *Trends Biomater. Artif. Organs* **2010**, *24*, 69–82.
2. Maier, P.; Hort, N. *Magnesium Alloys for Biomedical Applications*; Multidisciplinary Digital Publishing Institute: Basel, Switzerland, 2020.
3. Hanawa, T. In vivo metallic biomaterials and surface modification. *Mater. Sci. Eng.* **1999**, *267*, 260–266. [[CrossRef](#)]
4. Zhang, S. *Hydroxyapatite Coatings for Biomedical Applications*; CRC Press: Boca Raton, FL, USA, 2013.

5. Priyadarshini, B.; Rama, M.; Chetan; Vijayalakshmi, U. Bioactive coating as a surface modification technique for biocompatible metallic implants: A review. *J. Asian Ceram. Soc.* **2019**, *7*, 397–406. [[CrossRef](#)]
6. Jiang, J.; Han, G.; Zheng, X.; Chen, G.; Zhu, P. Characterization and biocompatibility study of hydroxyapatite coating on the surface of titanium alloy. *Surf. Coat. Technol.* **2019**, *375*, 645–651. [[CrossRef](#)]
7. Arcos, D.; Vallet-Regí, M. Substituted hydroxyapatite coatings of bone implants. *J. Mater. Chem. B* **2020**, *8*, 1781–1800. [[CrossRef](#)]
8. Niinomi, M. Recent metallic materials for biomedical applications. *Metall. Mater. Transactions A* **2002**, *33*, 477. [[CrossRef](#)]
9. Sridhar, T. Nanobioceramic coatings for biomedical applications. *Mater. Technol.* **2010**, *25*, 184–195. [[CrossRef](#)]
10. Francis, M.D.; Webb, N.C. Hydroxyapatite formation from a hydrated calcium monohydrogen phosphate precursor. *Calcif. Tissue Res.* **1970**, *6*, 335–342. [[CrossRef](#)]
11. Grafts, I.B.; Substitutes, B. Three-dimensionally engineered hydroxyapatite ceramics with interconnected pores as a bone substitute and tissue engineering scaffold. In *Biomaterials in Orthopedics*; Marcel Dekker, Inc.: New York, NY, USA, 2004.
12. Martin, R.; Brown, P. Mechanical properties of hydroxyapatite formed at physiological temperature. *J. Mater. Sci. Mater. Med.* **1995**, *6*, 138–143. [[CrossRef](#)]
13. Surmenev, R.A.; Surmeneva, M.A.; Ivanova, A.A. Significance of calcium phosphate coatings for the enhancement of new bone osteogenesis—a review. *Acta Biomater.* **2014**, *10*, 557–579. [[CrossRef](#)]
14. Prakasam, M.; Locs, J.; Salma-Ancane, K.; Loca, D.; Largeteau, A.; Berzina-Cimdina, L. Fabrication, properties and applications of dense hydroxyapatite: A review. *J. Funct. Biomater.* **2015**, *6*, 1099–1140. [[CrossRef](#)] [[PubMed](#)]
15. Lu, M.; Chen, H.; Yuan, B.; Zhou, Y.; Min, L.; Xiao, Z.; Zhu, X.; Tu, C.; Zhang, X. Electrochemical Deposition of Nanostructured Hydroxyapatite Coating on Titanium with Enhanced Early Stage Osteogenic Activity and Osseointegration. *Int. J. Nanomed.* **2020**, *15*, 6605. [[CrossRef](#)] [[PubMed](#)]
16. Sadat-Shojai, M.; Khorasani, M.-T.; Dinpanah-Khoshdargi, E.; Jamshidi, A. Synthesis methods for nanosized hydroxyapatite with diverse structures. *Acta Biomater.* **2013**, *9*, 7591–7621. [[CrossRef](#)] [[PubMed](#)]
17. Pandey, A.; Awasthi, A.; Saxena, K.K. Metallic implants with properties and latest production techniques: A review. *Adv. Mater. Process. Technol.* **2020**, *6*, 405–440. [[CrossRef](#)]
18. Prasad, K.; Bazaka, O.; Chua, M.; Rochford, M.; Fedrick, L.; Spoor, J.; Symes, R.; Tieppo, M.; Collins, C.; Cao, A. Metallic biomaterials: Current challenges and opportunities. *Materials* **2017**, *10*, 884. [[CrossRef](#)]
19. Awasthi, S.; Pandey, S.K.; Arunan, E.; Srivastava, C. A Review on Hydroxyapatite Coatings for Biomedical Application: Experimental and Theoretical Perspectives. *J. Mater. Chem. B* **2020**. [[CrossRef](#)]
20. Song, Y.; Shan, D.; Han, E.J. Electrodeposition of hydroxyapatite coating on AZ91D magnesium alloy for biomaterial application. *Mater. Lett.* **2008**, *62*, 3276–3279. [[CrossRef](#)]
21. Zhong, Z.; Qin, J.; Ma, J. Cellulose acetate/hydroxyapatite/chitosan coatings for improved corrosion resistance and bioactivity. *Mater. Sci. Eng. C* **2015**, *49*, 251–255. [[CrossRef](#)]
22. Surmenev, R.A.; Surmeneva, M.A. A critical review of decades of research on calcium-phosphate-based coatings: How far are we from their widespread clinical application? *Curr. Opin. Biomed. Eng.* **2019**, *10*, 35–44. [[CrossRef](#)]
23. Cizek, J.; Matejcek, J. Medicine Meets Thermal Spray Technology: A Review of Patents. *J. Therm. Spray Technol.* **2018**, *27*, 1251–1279. [[CrossRef](#)]
24. Mohseni, E.; Zalnezhad, E.; Bushroa, A.R. Comparative investigation on the adhesion of hydroxyapatite coating on Ti–6Al–4V implant: A review paper. *Int. J. Adhes. Adhes.* **2014**, *48*, 238–257. [[CrossRef](#)]
25. Lacefield, W. Hydroxyapatite coatings. *Ann. New York Acad. Sci.* **1988**, *523*, 72–80. [[CrossRef](#)] [[PubMed](#)]
26. Mahapatro, A. Bio-functional nano-coatings on metallic biomaterials. *Mater. Sci. Eng. C* **2015**, *55*, 227–251. [[CrossRef](#)] [[PubMed](#)]
27. Abu Bakar, M.; Cheng, M.; Tang, S.; Yu, S.; Liao, K.; Tan, C.; Khor, K.; Cheang, P. Tensile properties, tension–tension fatigue and biological response of polyetheretherketone–hydroxyapatite composites for load-bearing orthopedic implants. *Biomaterials* **2003**, *24*, 2245–2250. [[CrossRef](#)]
28. Roy, M.; Krishna, B.V.; Bandyopadhyay, A.; Bose, S. Laser processing of bioactive tricalcium phosphate coating on titanium for load-bearing implants. *Acta Biomater.* **2008**, *4*, 324–333. [[CrossRef](#)]
29. Kannan, M. Hydroxyapatite coating on biodegradable magnesium and magnesium-based alloys. In *Hydroxyapatite (HAp) for Biomedical Applications*; Elsevier: Amsterdam, The Netherlands, 2015; pp. 289–306.

30. Witte, F.; Feyerabend, F.; Maier, P.; Fischer, J.; Störmer, M.; Blawert, C.; Dietzel, W.; Hort, N. Biodegradable magnesium–hydroxyapatite metal matrix composites. *Biomaterials* **2007**, *28*, 2163–2174. [[CrossRef](#)]
31. Kezhi, L.; Qian, G.; Leilei, Z.; Yulei, Z.; Shoujie, L.; Kebing, G.; Shaoxian, L. Synthesis and characterization of Si-substituted hydroxyapatite bioactive coating for SiC-coated carbon/carbon composites. *Ceram. Int.* **2017**, *43*, 1410–1414. [[CrossRef](#)]
32. Ballarre, J.; López, D.A.; Schreiner, W.H.; Durán, A.; Ceré, S.M. Protective hybrid sol–gel coatings containing bioactive particles on surgical grade stainless steel: Surface characterization. *Appl. Surf. Sci.* **2007**, *253*, 7260–7264. [[CrossRef](#)]
33. Ballarre, J.; Manjubala, I.; Schreiner, W.H.; Orellano, J.C.; Fratzl, P.; Ceré, S. Improving the osteointegration and bone–implant interface by incorporation of bioactive particles in sol–gel coatings of stainless steel implants. *Acta Biomater.* **2010**, *6*, 1601–1609. [[CrossRef](#)]
34. Ballarre, J.; Seltzer, R.; Mendoza, E.; Orellano, J.C.; Mai, Y.-W.; García, C.; Ceré, S. Morphologic and nanomechanical characterization of bone tissue growth around bioactive sol–gel coatings containing wollastonite particles applied on stainless steel implants. *Mater. Sci. Eng. C* **2011**, *31*, 545–552. [[CrossRef](#)]
35. Hsieh, M.-F.; Perng, L.-H.; Chin, T.-S. Hydroxyapatite coating on Ti6Al4V alloy using a sol–gel derived precursor. *Mater. Chem. Phys.* **2002**, *74*, 245–250. [[CrossRef](#)]
36. Liu, D.-M.; Yang, Q.; Troczynski, T. Sol–gel hydroxyapatite coatings on stainless steel substrates. *Biomaterials* **2002**, *23*, 691–698. [[CrossRef](#)]
37. Stoch, A.; Jastrze, W.; Długoń, E.; Lejda, W.; Trybalska, B.; Stoch, G.; Adamczyk, A. Sol–gel derived hydroxyapatite coatings on titanium and its alloy Ti6Al4V. *J. Mol. Struct.* **2005**, *744*, 633–640. [[CrossRef](#)]
38. Wang, X.; Cai, S.; Liu, T.; Ren, M.; Huang, K.; Zhang, R.; Zhao, H. Fabrication and corrosion resistance of calcium phosphate glass-ceramic coated Mg alloy via a PEG assisted sol–gel method. *Ceram. Int.* **2014**, *40*, 3389–3398. [[CrossRef](#)]
39. Metikoš-Huković, M.; Tkalčec, E.; Kwokal, A.; Piljac, J. An in vitro study of Ti and Ti-alloys coated with sol–gel derived hydroxyapatite coatings. *Surf. Coat. Technol.* **2003**, *165*, 40–50. [[CrossRef](#)]
40. García, C.; Ceré, S.; Durán, A. Bioactive coatings prepared by sol–gel on stainless steel 316L. *J. Non-Cryst. Solids* **2004**, *348*, 218–224. [[CrossRef](#)]
41. Li, Y.; Li, Q.; Zhu, S.; Luo, E.; Li, J.; Feng, G.; Liao, Y.; Hu, J. The effect of strontium-substituted hydroxyapatite coating on implant fixation in ovariectomized rats. *Biomaterials* **2010**, *31*, 9006–9014. [[CrossRef](#)]
42. Zhang, J.; Guan, R.; Zhang, X. Synthesis and characterization of sol–gel hydroxyapatite coatings deposited on porous NiTi alloys. *J. Alloy. Compd.* **2011**, *509*, 4643–4648. [[CrossRef](#)]
43. Bryington, M.S.; Hayashi, M.; Kozai, Y.; VanDeWeghe, S.; Andersson, M.; Wennerberg, A.; Jimbo, R. The influence of nano hydroxyapatite coating on osseointegration after extended healing periods. *Dent. Mater.* **2013**, *29*, 514–520. [[CrossRef](#)]
44. Rojaee, R.; Fathi, M.; Raeissi, K. Controlling the degradation rate of AZ91 magnesium alloy via sol–gel derived nanostructured hydroxyapatite coating. *Mater. Sci. Eng. C* **2013**, *33*, 3817–3825. [[CrossRef](#)]
45. Catauro, M.; Bollino, F.; Papale, F.; Lamanna, G. TiO₂/PCL Hybrid Layers Prepared via Sol-Gel Dip Coating for the Surface Modification of Titanium Implants: Characterization and Bioactivity Evaluation. *Appl. Mech. Mater.* **2015**, *760*, 353–358. [[CrossRef](#)]
46. Fu, T.; Sun, J.-M.; Alajmi, Z.; Wu, F. Sol-gel preparation, corrosion resistance and hydrophilicity of Ta-containing TiO₂ films on Ti6Al4V alloy. *Trans. Nonferrous Met. Soc. China* **2015**, *25*, 471–476. [[CrossRef](#)]
47. Zhao, H.; Cai, S.; Niu, S.; Zhang, R.; Wu, X.; Xu, G.; Ding, Z. The influence of alkali pretreatments of AZ31 magnesium alloys on bonding of bioglass–ceramic coatings and corrosion resistance for biomedical applications. *Ceram. Int.* **2015**, *41*, 4590–4600. [[CrossRef](#)]
48. Ma, M.; Ye, W.; Wang, X.X. Effect of supersaturation on the morphology of hydroxyapatite crystals deposited by electrochemical deposition on titanium. *Mater. Lett.* **2008**, *62*, 3875–3877. [[CrossRef](#)]
49. Wang, H.; Eliaz, N.; Xiang, Z.; Hsu, H.-P.; Spector, M.; Hobbs, L.W. Early bone apposition in vivo on plasma-sprayed and electrochemically deposited hydroxyapatite coatings on titanium alloy. *Biomater.* **2006**, *27*, 4192–4203. [[CrossRef](#)]
50. Qiu, D.; Wang, A.; Yin, Y. Characterization and corrosion behavior of hydroxyapatite/zirconia composite coating on NiTi fabricated by electrochemical deposition. *Appl. Surf. Sci.* **2010**, *257*, 1774–1778. [[CrossRef](#)]
51. Wang, L.-N.; Luo, J.-L. Preparation of hydroxyapatite coating on CoCrMo implant using an effective electrochemically-assisted deposition pretreatment. *Mater. Charact.* **2011**, *62*, 1076–1086. [[CrossRef](#)]

52. Qiu, D.; Yang, L.; Yin, Y.; Wang, A. Preparation and characterization of hydroxyapatite/titania composite coating on NiTi alloy by electrochemical deposition. *Surf. Coat. Technol.* **2011**, *205*, 3280–3284. [[CrossRef](#)]
53. Rad, A.T.; Solati-Hashjin, M.; Abu Osman, N.A.; Faghihi, S. Improved bio-physical performance of hydroxyapatite coatings obtained by electrophoretic deposition at dynamic voltage. *Ceram. Int.* **2014**, *40*, 12681–12691. [[CrossRef](#)]
54. Rojaee, R.; Fathi, M.; Raeissi, K.; Sharifnabi, A. Biodegradation assessment of nanostructured fluoridated hydroxyapatite coatings on biomedical grade magnesium alloy. *Ceram. Int.* **2014**, *40*, 15149–15158. [[CrossRef](#)]
55. Sun, G.; Ma, J.; Zhang, S. Electrophoretic deposition of zinc-substituted hydroxyapatite coatings. *Mater. Sci. Eng. C* **2014**, *39*, 67–72. [[CrossRef](#)] [[PubMed](#)]
56. Bigi, A.; Boanini, E.; Bracci, B.; Facchini, A.; Panzavolta, S.; Segatti, F.; Sturba, L. Nanocrystalline hydroxyapatite coatings on titanium: A new fast biomimetic method. *Biomaterials* **2005**, *26*, 4085–4089. [[CrossRef](#)] [[PubMed](#)]
57. Schrooten, J.; Helsen, J. Adhesion of bioactive glass coating to Ti6Al4V oral implant. *Biomaterials* **2000**, *21*, 1461–1469. [[CrossRef](#)]
58. Yang, Y.; Ong, J.L.; Tian, J. Deposition of highly adhesive ZrO(2) coating on Ti and CoCrMo implant materials using plasma spraying. *Biomaterials* **2003**, *24*, 619–627. [[CrossRef](#)]
59. Yang, Y.; Chou, B. Bonding strength investigation of plasma-sprayed HA coatings on alumina substrate with porcelain intermediate layer. *Mater. Chem. Phys.* **2007**, *104*, 312–319. [[CrossRef](#)]
60. Grandfield, K.; Palmquist, A.; Goncalves, S.; Taylor, A.; Taylor, M.; Emanuelsson, L.; Thomsen, P.; Engqvist, H. Free form fabricated features on CoCr implants with and without hydroxyapatite coating in vivo: A comparative study of bone contact and bone growth induction. *J. Mater. Sci. Mater. Electron.* **2011**, *22*, 899–906. [[CrossRef](#)]
61. Vencel, A.; Arostegui, S.; Favaro, G.; Zivic, F.; Mrdak, M.; Mitrović, S.; Popovic, V. Evaluation of adhesion/cohesion bond strength of the thick plasma spray coatings by scratch testing on coatings cross-sections. *Tribol. Int.* **2011**, *44*, 1281–1288. [[CrossRef](#)]
62. Hung, K.-Y.; Lo, S.-C.; Shih, C.-S.; Yang, Y.-C.; Feng, H.-P.; Lin, Y.-C. Titanium surface modified by hydroxyapatite coating for dental implants. *Surf. Coat. Technol.* **2013**, *231*, 337–345. [[CrossRef](#)]
63. Latifi, A.; Imani, M.; Khorasani, M.T.; Joupari, M.D. Plasma surface oxidation of 316L stainless steel for improving adhesion strength of silicone rubber coating to metal substrate. *Appl. Surf. Sci.* **2014**, *320*, 471–481. [[CrossRef](#)]
64. Hameed, P.; Gopal, V.; Bjorklund, S.; Ganvir, A.; Sen, D.; Markocsan, N.; Manivasagam, G. Axial suspension plasma spraying: An ultimate technique to tailor Ti6Al4V surface with HAp for orthopaedic applications. *Colloids Surf. B: Biointerfaces* **2019**, *173*, 806–815. [[CrossRef](#)]
65. Yang, Y.; Kim, K.-H.; Ong, J.L. A review on calcium phosphate coatings produced using a sputtering process?an alternative to plasma spraying. *Biomaterials* **2005**, *26*, 327–337. [[CrossRef](#)] [[PubMed](#)]
66. Rauch, J.; Bolelli, G.; Killinger, A.; Gadow, R.; Cannillo, V.; Lusvarghi, L. Advances in High Velocity Suspension Flame Spraying (HVSFS). *Surf. Coat. Technol.* **2009**, *203*, 2131–2138. [[CrossRef](#)]
67. Bolelli, G.; Bellucci, D.; Cannillo, V.; Lusvarghi, L.; Sola, A.; Stiegler, N.; Müller, P.; Killinger, A.; Gadow, R.; Altomare, L.; et al. Suspension thermal spraying of hydroxyapatite: Microstructure and in vitro behaviour. *Mater. Sci. Eng. C* **2014**, *34*, 287–303. [[CrossRef](#)] [[PubMed](#)]
68. Bolelli, G.; Bellucci, D.; Cannillo, V.; Gadow, R.; Killinger, A.; Lusvarghi, L.; Müller, P.; Sola, A. Comparison between Suspension Plasma Sprayed and High Velocity Suspension Flame Sprayed bioactive coatings. *Surf. Coat. Technol.* **2015**, *280*, 232–249. [[CrossRef](#)]
69. Clèries, L.; Martínez, E.; Fernández-Pradas, J.; Sardin, G.; Esteve, J.; Morenza, J. Mechanical properties of calcium phosphate coatings deposited by laser ablation. *Biomaterials* **2000**, *21*, 967–971. [[CrossRef](#)]
70. Fernández-Pradas, J.; Clèries, L.; Martínez, E.; Sardin, G.; Esteve, J.; Morenza, J. Influence of thickness on the properties of hydroxyapatite coatings deposited by KrF laser ablation. *Biomaterials* **2001**, *22*, 2171–2175. [[CrossRef](#)]
71. Khandelwal, H.; Singh, G.; Agrawal, K.; Prakash, S.; Agarwal, R. Characterization of hydroxyapatite coating by pulse laser deposition technique on stainless steel 316 L by varying laser energy. *Appl. Surf. Sci.* **2013**, *265*, 30–35. [[CrossRef](#)]

72. Li, J.; Liao, H.; Hermansson, L. Sintering of partially-stabilized zirconia and partially-stabilized zirconia—hydroxyapatite composites by hot isostatic pressing and pressureless sintering. *Biomaterials* **1996**, *17*, 1787–1790. [[CrossRef](#)]
73. Onoki, T.; Hashida, T. New method for hydroxyapatite coating of titanium by the hydrothermal hot isostatic pressing technique. *Surf. Coat. Technol.* **2006**, *200*, 6801–6807. [[CrossRef](#)]
74. Das, B.; Bandyopadhyay, P.; Nath, A.K. An investigation on corrosion resistance and mechanical properties of laser remelted flame sprayed coating. *Adv. Mater. Process. Technol.* **2018**, *4*, 1–9. [[CrossRef](#)]
75. Monsalve, M.; Lopez, E.; Ageorges, H.; Vargas, F. Bioactivity and mechanical properties of bioactive glass coatings fabricated by flame spraying. *Surf. Coat. Technol.* **2015**, *268*, 142–146. [[CrossRef](#)]
76. Surmenev, R.A. A review of plasma-assisted methods for calcium phosphate-based coatings fabrication. *Surf. Coat. Technol.* **2012**, *206*, 2035–2056. [[CrossRef](#)]
77. Qu, J.; Ouyang, L.; Kuo, C.-C.; Martin, D. Stiffness, strength and adhesion characterization of electrochemically deposited conjugated polymer films. *Acta Biomater.* **2016**, *31*, 114–121. [[CrossRef](#)] [[PubMed](#)]
78. Say, Y.; Aksakal, B.; Dikici, B. Effect of hydroxyapatite/SiO₂ hybride coatings on surface morphology and corrosion resistance of REX-734 alloy. *Ceram. Int.* **2016**, *42*, 10151–10158. [[CrossRef](#)]
79. Fomin, A.; Fomina, M.; Koshuro, V.; Rodionov, I.; Zakharevich, A.; Skaptsov, A. Structure and mechanical properties of hydroxyapatite coatings produced on titanium using plasma spraying with induction preheating. *Ceram. Int.* **2017**, *43*, 11189–11196. [[CrossRef](#)]
80. Mohseni, E.; Zalnezhad, E.; Bushroa, A.; Hamouda, A.M.; Goh, B.; Yoon, G.H. Ti/TiN/HA coating on Ti-6Al-4V for biomedical applications. *Ceram. Int.* **2015**, *41*, 14447–14457. [[CrossRef](#)]
81. Packham, D.E. Surface energy, surface topography and adhesion. *Int. J. Adhes. Adhes.* **2003**, *23*, 437–448. [[CrossRef](#)]
82. Huang, Y.; Zhang, X.; Zhang, H.; Qiao, H.; Zhang, X.; Jia, T.; Han, S.; Gao, Y.; Xiao, H.; Yang, H.J. Fabrication of silver- and strontium-doped hydroxyapatite/TiO₂ nanotube bilayer coatings for enhancing bactericidal effect and osteoinductivity. *Ceram. Int.* **2017**, *43*, 992–1007. [[CrossRef](#)]
83. Mahjoubi, H.; Buck, E.; Manimunda, P.; Farivar, R.; Chromik, R.; Murshed, M.; Cerruti, M. Surface phosphonation enhances hydroxyapatite coating adhesion on polyetheretherketone and its osseointegration potential. *Acta Biomater.* **2017**, *47*, 149–158. [[CrossRef](#)]
84. Bauer, S.; Schmuki, P.; Von Der Mark, K.; Park, J. Engineering biocompatible implant surfaces: Part I: Materials and surfaces. *Prog. Mater. Sci.* **2013**, *58*, 261–326. [[CrossRef](#)]
85. Tao, Y.; Ke, G.; Xie, Y.; Chen, Y.; Shi, S.; Guo, H. Adhesion strength and nucleation thermodynamics of four metals (Al, Cu, Ti, Zr) on AlN substrates. *Appl. Surf. Sci.* **2015**, *357*, 8–13. [[CrossRef](#)]
86. Huang, Y.; Hao, M.; Nian, X.; Qiao, H.; Zhang, X.; Zhang, X.; Song, G.; Guo, J.; Pang, X.; Zhang, H. Strontium and copper co-substituted hydroxyapatite-based coatings with improved antibacterial activity and cytocompatibility fabricated by electrodeposition. *Ceram. Int.* **2016**, *42*, 11876–11888. [[CrossRef](#)]
87. Zhao, Z.; Du, L.; Tao, Y.; Li, Q.; Luo, L. Enhancing the adhesion strength of micro electroforming layer by ultrasonic agitation method and the application. *Ultrason. Sonochemistry* **2016**, *33*, 10–17. [[CrossRef](#)] [[PubMed](#)]
88. Hannink, G.; Arts, J.C. Bioresorbability, porosity and mechanical strength of bone substitutes: What is optimal for bone regeneration? *Injury* **2011**, *42*, S22–S25. [[CrossRef](#)] [[PubMed](#)]
89. Mediaswanti, K.; Wen, C.; Ivanova, E.; Berndt, C.; Malherbe, F.; Pham, V.; Wang, J. A review on bioactive porous metallic biomaterials. *J. Biomim. Biomater. Tissue Eng.* **2013**, *18*, 1–8.
90. Berndt, C.C.; Hasan, F.; Tietz, U.; Schmitz, K.-P. A Review of Hydroxyapatite Coatings Manufactured by Thermal Spray. In *Springer Series in Biomaterials Science and Engineering*; Springer Science and Business Media LLC: Larkspur, CA, USA, 2014; pp. 267–329.
91. Ma, J.; Wang, C.; Ban, C.; Chen, C.; Zhang, H. Pulsed laser deposition of magnesium-containing bioactive glass film on porous Ti-6Al-4V substrate pretreated by micro-arc oxidation. *Vacuum* **2016**, *125*, 48–55. [[CrossRef](#)]
92. Almeida, R.M.; Gama, A.; Vueva, Y. Bioactive sol–gel scaffolds with dual porosity for tissue engineering. *J. Sol.-Gel Sci. Technol.* **2011**, *57*, 336–342. [[CrossRef](#)]
93. MI, Z.R.; Shuib, S.; Hassan, A.; Shorki, A.; Ibrahim, M.M. Problem of Stress Shielding and Improvement to the Hip Implat Designs: A Review. *J. Med. Sci.* **2007**, *7*, 460–467.

94. Bugbee, W.D.; Sychterz, C.J.; Engh, C.A. Bone Remodeling Around Cementless Hip Implants. *South. Med. J.* **1996**, *89*, 1036–1040. [[CrossRef](#)]
95. Bellucci, D.; Veronesi, E.; Strusi, V.; Petrachi, T.; Murgia, A.; Mastroli, I.; Dominici, M.; Cannillo, V. Human Mesenchymal Stem Cell Combined with a New Strontium-Enriched Bioactive Glass: An ex-vivo Model for Bone Regeneration. *Materials* **2019**, *12*, 3633. [[CrossRef](#)]
96. Yuan, Q.; Golden, T.D. Electrochemical study of hydroxyapatite coatings on stainless steel substrates. *Thin Solid Film.* **2009**, *518*, 55–60. [[CrossRef](#)]
97. Suwanprateeb, J.; Suvannapruk, W.; Chokevivat, W.; Kiertykritikhon, S.; Jaruwangsanti, N.; Tienboon, P. Bioactivity of a sol-gel-derived hydroxyapatite coating on titanium implants in vitro and in vivo. *Asian Biomed.* **2018**, *12*, 35–44. [[CrossRef](#)]
98. Zhang, S.; Xianting, Z.; Yongsheng, W.; Kui, C.; Wenjian, W. Adhesion strength of sol-gel derived fluoridated hydroxyapatite coatings. *Surf. Coat. Technol.* **2006**, *200*, 6350–6354. [[CrossRef](#)]
99. Combes, C.; Rey, C. Amorphous calcium phosphates: Synthesis, properties and uses in biomaterials. *Acta Biomater.* **2010**, *6*, 3362–3378. [[CrossRef](#)]
100. Costa, D.O.; Dixon, S.J.; Rizkalla, A.S. One- and Three-Dimensional Growth of Hydroxyapatite Nanowires during Sol-Gel-Hydrothermal Synthesis. *ACS Appl. Mater. Interfaces* **2012**, *4*, 1490–1499. [[CrossRef](#)]
101. Liu, D.-M.; Troczynski, T.; Tseng, W.J. Water-based sol-gel synthesis of hydroxyapatite: Process development. *Biomaterials* **2001**, *22*, 1721–1730. [[CrossRef](#)]
102. Cardoso, D.A.; Jansen, J.A.; Leeuwenburgh, S.C.G. Synthesis and application of nanostructured calcium phosphate ceramics for bone regeneration. *J. Biomed. Mater. Res. Part. B: Appl. Biomater.* **2012**, *100*, 2316–2326. [[CrossRef](#)]
103. Choi, A.H.; Ben-Nissan, B. Sol-gel production of bioactive nanocoatings for medical applications. Part II: Current research and development. *Nanomedicine* **2007**, *2*, 51–61. [[CrossRef](#)]
104. Davar, F.; Shayan, N. Preparation of zirconia-magnesia nanocomposite powders and coating by a sucrose mediated sol-gel method and investigation of its corrosion behavior. *Ceram. Int.* **2017**, *43*, 3384–3392. [[CrossRef](#)]
105. Shadanbaz, S.; Dias, G.J. Calcium phosphate coatings on magnesium alloys for biomedical applications: A review. *Acta Biomater.* **2012**, *8*, 20–30. [[CrossRef](#)]
106. Qu, H.; Wei, M. Improvement of bonding strength between biomimetic apatite coating and substrate. *J. Biomed. Mater. Res. Part. B Appl. Biomater.* **2008**, *84*, 436–443. [[CrossRef](#)] [[PubMed](#)]
107. Bakan, F.; Laçin, O.; Saraç, H. A novel low temperature sol-gel synthesis process for thermally stable nano crystalline hydroxyapatite. *Powder Technol.* **2013**, *233*, 295–302. [[CrossRef](#)]
108. Catauro, M.; Bollino, F.; Papale, F.; Ferrara, C.; Mustarelli, P. Silica-polyethylene glycol hybrids synthesized by sol-gel: Biocompatibility improvement of titanium implants by coating. *Mater. Sci. Eng. C* **2015**, *55*, 118–125. [[CrossRef](#)] [[PubMed](#)]
109. Dorozhkin, S.V. Calcium orthophosphate deposits: Preparation, properties and biomedical applications. *Mater. Sci. Eng. C* **2015**, *55*, 272–326. [[CrossRef](#)] [[PubMed](#)]
110. Guo, L.; Li, H. Fabrication and characterization of thin nano-hydroxyapatite coatings on titanium. *Surf. Coat. Technol.* **2004**, *185*, 268–274. [[CrossRef](#)]
111. Motealleh, A.; Eqtesadi, S.; Perera, F.H.; Pajares, A.; Guiberteau, F.; González, P.M. Understanding the role of dip-coating process parameters in the mechanical performance of polymer-coated bioglass robocast scaffolds. *J. Mech. Behav. Biomed. Mater.* **2016**, *64*, 253–261. [[CrossRef](#)] [[PubMed](#)]
112. Hornberger, H.; Virtanen, S.; Boccaccini, A.J.A.b. Biomedical coatings on magnesium alloys—a review. *Acta Biomater.* **2012**, *8*, 2442–2455. [[CrossRef](#)]
113. Yusoff, M.F.M.; Kadir, M.R.A.; Iqbal, N.; Hassan, M.A.; Hussain, R. Dipcoating of poly (ϵ -caprolactone)/hydroxyapatite composite coating on Ti6Al4V for enhanced corrosion protection. *Surf. Coat. Technol.* **2014**, *245*, 102–107. [[CrossRef](#)]
114. Yuan, J.; Zhao, K.; Cai, T.; Gao, Z.; Yang, L.; He, D. One-step dip-coating of uniform γ -Al₂O₃ layers on cordierite honeycombs and its environmental applications. *Ceram. Int.* **2016**, *42*, 14384–14390. [[CrossRef](#)]
115. Catauro, M.; Bollino, F.; Papale, F.; Giovanardi, R.; Veronesi, P. Corrosion behavior and mechanical properties of bioactive sol-gel coatings on titanium implants. *Mater. Sci. Eng. C* **2014**, *43*, 375–382. [[CrossRef](#)]
116. Gray, J.; Luan, B. Protective coatings on magnesium and its alloys—A critical review. *J. Alloy Compd.* **2002**, *336*, 88–113. [[CrossRef](#)]

117. Dinda, G.; Shin, J.; Mazumder, J. Pulsed laser deposition of hydroxyapatite thin films on Ti-6Al-4V: Effect of heat treatment on structure and properties. *Acta Biomater.* **2009**, *5*, 1821–1830. [[CrossRef](#)] [[PubMed](#)]
118. Shimizu, T.; Fujibayashi, S.; Yamaguchi, S.; Yamamoto, K.; Otsuki, B.; Takemoto, M.; Tsukanaka, M.; Kizuki, T.; Matsushita, T.; Kokubo, T.; et al. Bioactivity of sol-gel-derived TiO₂ coating on polyetheretherketone: In vitro and in vivo studies. *Acta Biomater.* **2016**, *35*, 305–317. [[CrossRef](#)] [[PubMed](#)]
119. Kim, H.-W.; Koh, Y.-H.; Li, L.-H.; Lee, S.; Kim, H.-E. Hydroxyapatite coating on titanium substrate with titania buffer layer processed by sol-gel method. *Biomaterials* **2004**, *25*, 2533–2538. [[CrossRef](#)] [[PubMed](#)]
120. Usinskas, P.; Stankeviciute, Z.; Beganskiene, A.; Kareiva, A. Sol-gel derived porous and hydrophilic calcium hydroxyapatite coating on modified titanium substrate. *Surf. Coat. Technol.* **2016**, *307*, 935–940. [[CrossRef](#)]
121. Kokubo, T.; Kushitani, H.; Sakka, S.; Kitsugi, T.; Yamamuro, T. Solutions able to reproduce in vivo surface-structure changes in bioactive glass-ceramic A-W3. *J. Biomed. Mater. Res.* **1990**, *24*, 721–734. [[CrossRef](#)]
122. Mali, S.A.; Nune, K.; Misra, R.D.K. Biomimetic nanostructured hydroxyapatite coatings on metallic implant materials. *Mater. Technol.* **2016**, *31*, 782–790. [[CrossRef](#)]
123. Escada, A.L.; Machado, J.P.B.; Schneider, S.G.; Alves-Rezende, M.C.R.; Claro, A.P.R.A. Biomimetic calcium phosphate coating on Ti-7.5Mo alloy for dental application. *J. Mater. Sci. Mater. Electron.* **2011**, *22*, 2457–2465. [[CrossRef](#)]
124. Stigter, M.; De Groot, K.; Layrolle, P. Incorporation of tobramycin into biomimetic hydroxyapatite coating on titanium. *Biomaterials* **2002**, *23*, 4143–4153. [[CrossRef](#)]
125. Bharati, S.; Sinha, M.K.; Basu, D. Hydroxyapatite coating by biomimetic method on titanium alloy using concentrated SBF. *Bull. Mater. Sci.* **2005**, *28*, 617–621. [[CrossRef](#)]
126. Arrés, M.; Salama, M.; Rechená, D.; Paradiso, P.; Reis, L.; Alves, M.M.; Rego, A.M.B.D.; Carmezim, M.J.; Vaz, M.F.; Deus, A.; et al. Surface and mechanical properties of a nanostructured citrate hydroxyapatite coating on pure titanium. *J. Mech. Behav. Biomed. Mater.* **2020**, *108*, 103794. [[CrossRef](#)] [[PubMed](#)]
127. Habibovic, P.; Barrère, F.; Van Blitterswijk, C.; Groot, K.; Layrolle, P. Biomimetic Hydroxyapatite Coating on Metal Implants. *J. Am. Ceram. Soc.* **2004**, *85*, 517–522. [[CrossRef](#)]
128. Xie, J.; Luan, B. Formation of hydroxyapatite coating using novel chemo-biomimetic method. *J. Mater. Sci. Mater. Electron.* **2008**, *19*, 3211–3220. [[CrossRef](#)] [[PubMed](#)]
129. Nazir, M.; Ting, O.P.; Yee, T.S.; Pushparajan, S.; Swaminathan, D.; Kutty, M.G. Biomimetic Coating of Modified Titanium Surfaces with Hydroxyapatite Using Simulated Body Fluid. *Adv. Mater. Sci. Eng.* **2015**, *2015*, 407379. [[CrossRef](#)]
130. Gunputh, U.F.; Le, H. A Review of In-Situ Grown Nanocomposite Coatings for Titanium Alloy Implants. *J. Compos. Sci.* **2020**, *4*, 41. [[CrossRef](#)]
131. Goto, T.; Katsui, H. Chemical vapor deposition of Ca-P-O film coating. In *Interface Oral Health Science 2014*; Springer: New York, NY, USA, 2015; pp. 103–115.
132. Cabañas, M.V.; Vallet-Regí, M. Calcium phosphate coatings deposited by aerosol chemical vapour deposition. *J. Mater. Chem.* **2003**, *13*, 1104–1107. [[CrossRef](#)]
133. Gao, Y. Synthesis and Characterization of Calcium Phosphate Coatings by Metalorganic Chemical Vapor Deposition. In *Proceedings of the MRS Proceedings*; Cambridge University Press (CUP): Cambridge, UK, 1998; Volume 550, p. 550.
134. Darr, J.; Guo, Z.X.; Raman, V.; Bououdina, M.; Rehman, I.U. Metal organic chemical vapour deposition (MOCVD) of bone mineral like carbonated hydroxyapatite coatings. Electronic supplementary information (ESI) available: Experimental data. *Chem. Commun.* **2004**, 696. [[CrossRef](#)]
135. Sato, M.; Tu, R.; Goto, T.; Ueda, K.; Narushima, T. Hydroxyapatite Formation on CaTiO₃ Film Prepared by Metal-Organic Chemical Vapor Deposition. *Mater. Trans.* **2007**, *48*, 1505–1510. [[CrossRef](#)]
136. Tsutsumi, H.; Niinomi, M.; Nakai, M.; Gozawa, T.; Akahori, T.; Saito, K.; Tu, R.; Goto, T. Fabrication of Hydroxyapatite Film on Ti-29Nb-13Ta-4.6Zr Using a MOCVD Technique. *Mater. Trans.* **2010**, *51*, 2277–2283. [[CrossRef](#)]
137. Zhitomirsky, I. Cathodic electrodeposition of ceramic and organoceramic materials. *Fundam. Asp.* **2002**, *97*, 279–317.
138. Li, T.-T.; Ling, L.; Lin, M.-C.; Peng, H.-K.; Ren, H.-T.; Lou, C.-W.; Lin, J.-H. Recent advances in multifunctional hydroxyapatite coating by electrochemical deposition. *J. Mater. Sci.* **2020**, *55*, 6352–6374. [[CrossRef](#)]

139. Sobolev, A.; Valkov, A.; Kossenko, A.; Wolicki, I.; Zinigrad, M.; Borodianskiy, K. Bioactive Coating on Ti Alloy with High Osseointegration and Antibacterial Ag Nanoparticles. *ACS Appl. Mater. Interfaces* **2019**, *11*, 39534–39544. [[CrossRef](#)] [[PubMed](#)]
140. Nuswantoro, N.F.; Budiman, I.; Septiawarman, A.; Tjong, D.H.; Manjas, M. Gunawarman Effect of Applied Voltage and Coating Time on Nano Hydroxyapatite Coating on Titanium Alloy Ti6Al4V Using Electrophoretic Deposition for Orthopaedic Implant Application. In *IOP Conference Series: Materials Science and Engineering*; IOP Publishing: Bristol, UK, 2019; Volume 547, p. 012004.
141. Fadli, A.; Komalasari; Indriyani, I. Coating Hydroxyapatite on 316L Stainless Steel Using Electroforesis Deposition Method. In *Journal of Physics: Conference Series*; IOP Publishing: Bristol, UK, 2019; Volume 1351, p. 012015.
142. He, D.-H.; Wang, P.; Liu, P.; Liu, X.; Ma, F.-C.; Zhao, J. HA coating fabricated by electrochemical deposition on modified Ti6Al4V alloy. *Surf. Coat. Technol.* **2016**, *301*, 6–12. [[CrossRef](#)]
143. Eliaz, N.; Shmueli, S.; Shur, I.; Benayahu, D.; Aronov, D.; Rosenman, G. The effect of surface treatment on the surface texture and contact angle of electrochemically deposited hydroxyapatite coating and on its interaction with bone-forming cells. *Acta Biomater.* **2009**, *5*, 3178–3191. [[CrossRef](#)] [[PubMed](#)]
144. Zhang, Y.-Y.; Tao, J.; Pang, Y.-C.; Wang, W.; Wang, T. Electrochemical deposition of hydroxyapatite coatings on titanium. *Trans. Nonferrous Met. Soc. China* **2006**, *16*, 633–637. [[CrossRef](#)]
145. Eliaz, N.; Sridhar, T.; Mudali, U.K.; Raj, B. Electrochemical and electrophoretic deposition of hydroxyapatite for orthopaedic applications. *Surf. Eng.* **2005**, *21*, 238–242. [[CrossRef](#)]
146. Li, T.-T.; Ling, L.; Lin, M.-C.; Jiang, Q.; Lin, J.; Lin, J.; Lou, C. Properties and Mechanism of Hydroxyapatite Coating Prepared by Electrodeposition on a Braid for Biodegradable Bone Scaffolds. *Nanomaterials* **2019**, *9*, 679. [[CrossRef](#)]
147. Isa, N.N.C.; Mohd, Y.; Yury, N. Electrochemical Deposition and Characterization of Hydroxyapatite (HAp) on Titanium Substrate. *Apchee Procedia* **2012**, *3*, 46–52. [[CrossRef](#)]
148. Parcharoen, Y.; Kajitvichyanukul, P.; Sirivisoot, S.; Termsuksawad, P. Hydroxyapatite electrodeposition on anodized titanium nanotubes for orthopedic applications. *Appl. Surf. Sci.* **2014**, *311*, 54–61. [[CrossRef](#)]
149. Li’Nan, J.; Chenghao, L.; Naibao, H.; Feng, D.; Lixia, W. Formation and Characterization of Hydroxyapatite Coating Prepared by Pulsed Electrochemical Deposition. *Rare Met. Mater. Eng.* **2015**, *44*, 592–598. [[CrossRef](#)]
150. Cotrut, C.M.; Vladescu, A.; Dinu, M.; Vranceanu, D.M. Influence of deposition temperature on the properties of hydroxyapatite obtained by electrochemical assisted deposition. *Ceram. Int.* **2018**, *44*, 669–677. [[CrossRef](#)]
151. Kwok, C.; Wong, P.; Cheng, F.; Man, H. Characterization and corrosion behavior of hydroxyapatite coatings on Ti6Al4V fabricated by electrophoretic deposition. *Appl. Surf. Sci.* **2009**, *255*, 6736–6744. [[CrossRef](#)]
152. Yang, G.-L.; He, F.-M.; Hu, J.-A.; Wang, X.-X.; Zhao, S.-F. Biomechanical Comparison of Biomimetically and Electrochemically Deposited Hydroxyapatite-Coated Porous Titanium Implants. *J. Oral Maxillofac. Surg.* **2010**, *68*, 420–427. [[CrossRef](#)]
153. Ayu, H.M.; Izman, S.; Daud, R.; Krishnamurthy, G.; Shah, A.; Tomadi, S.; Salwani, M.S. Surface Modification on CoCrMo Alloy to Improve the Adhesion Strength of Hydroxyapatite Coating. *Procedia Eng.* **2017**, *184*, 399–408. [[CrossRef](#)]
154. Catauro, M.; Bollino, F.; Giovanardi, R.; Veronesi, P. Modification of Ti6Al4V implant surfaces by biocompatible TiO₂/PCL hybrid layers prepared via sol–gel dip coating: Structural characterization, mechanical and corrosion behavior. *Mater. Sci. Eng. C* **2017**, *74*, 501–507. [[CrossRef](#)] [[PubMed](#)]
155. Khanal, S.; Mahfuz, H.; Rondinone, A.J.; Leventouri, T. Improvement of the fracture toughness of hydroxyapatite (HAp) by incorporation of carboxyl functionalized single walled carbon nanotubes (CfSWCNTs) and nylon. *Mater. Sci. Eng. C* **2016**, *60*, 204–210. [[CrossRef](#)] [[PubMed](#)]
156. Manonmani, R.; Vinodhini, S.P.; Venkatachalapathy, B.; Sridhar, T.M. Electrochemical, mechanical and osseointegration evaluation of NBPC-coated 316L SS by EPD. *Surf. Eng.* **2017**, *34*, 511–519. [[CrossRef](#)]
157. Supriadi, S.; Putri, S.L.; Ramadhan, R.; Suharno, B. Alkali-Heat Treatment of Ti-6Al-4V to Hydroxyapatite Coating Using Electrophoretic Method. *Key Eng. Mater.* **2020**, *846*, 175–180. [[CrossRef](#)]
158. Rath, P.C.; Besra, L.; Singh, B.P.; Bhattacharjee, S. Titania/hydroxyapatite bi-layer coating on Ti metal by electrophoretic deposition: Characterization and corrosion studies. *Ceram. Int.* **2012**, *38*, 3209–3216. [[CrossRef](#)]

159. Albayrak, O.; El-Atwani, O.; Altintas, S. Hydroxyapatite coating on titanium substrate by electrophoretic deposition method: Effects of titanium dioxide inner layer on adhesion strength and hydroxyapatite decomposition. *Surf. Coat. Technol.* **2008**, *202*, 2482–2487. [[CrossRef](#)]
160. Gadow, R.; Killinger, A.; Stiegler, N. Hydroxyapatite coatings for biomedical applications deposited by different thermal spray techniques. *Surf. Coat. Technol.* **2010**, *205*, 1157–1164. [[CrossRef](#)]
161. Heimann, R.B. Structure, properties, and biomedical performance of osteoconductive bioceramic coatings. *Surf. Coat. Technol.* **2013**, *233*, 27–38. [[CrossRef](#)]
162. Saadati, A.; Hesarikia, H.; Nourani, M.R.; Taheri, R.A. Electrophoretic deposition of hydroxyapatite coating on biodegradable Mg–4Zn–4Sn–0.6 Ca–0.5 Mn alloy. *Surf. Eng.* **2019**, *36*, 908–918. [[CrossRef](#)]
163. Santos, M.; Santos, C.; Carmezim, M.J. Production of bioactive hydroxyapatite coating by coblast process for orthopedic implants. In Proceedings of the 2019 IEEE 6th Portuguese Meeting on Bioengineering (ENBENG); Institute of Electrical and Electronics Engineers (IEEE), Lisbon, Portugal, 22–23 February 2019; pp. 1–4.
164. Morks, M.F. Fabrication and characterization of plasma-sprayed HA/SiO₂ coatings for biomedical application. *J. Mech. Behav. Biomed. Mater.* **2008**, *1*, 105–111. [[CrossRef](#)] [[PubMed](#)]
165. Fauchais, P.; Vardelle, A. Innovative and emerging processes in plasma spraying: From micro- to nano-structured coatings. *J. Phys. D Appl. Phys.* **2011**, *44*. [[CrossRef](#)]
166. Ročňáková, I.; Slámečka, K.; Montufar, E.; Remešová, M.; Dyčková, L.; Břínek, A.; Jech, D.; Dvořák, K.; Čelko, L.; Kaiser, J. Deposition of hydroxyapatite and tricalcium phosphate coatings by suspension plasma spraying: Effects of torch speed. *J. Eur. Ceram. Soc.* **2018**, *38*, 5489–5496. [[CrossRef](#)]
167. Bakshi, S.R.; Singh, V.; Seal, S.; Agarwal, A. Aluminum composite reinforced with multiwalled carbon nanotubes from plasma spraying of spray dried powders. *Surf. Coat. Technol.* **2009**, *203*, 1544–1554. [[CrossRef](#)]
168. Levingstone, T.J.; Ardhaoui, M.; Benyounis, K.; Looney, L.; Stokes, J.T. Plasma sprayed hydroxyapatite coatings: Understanding process relationships using design of experiment analysis. *Surf. Coat. Technol.* **2015**, *283*, 29–36. [[CrossRef](#)]
169. Fielding, G.A.; Roy, M.; Bandyopadhyay, A.; Bose, S. Antibacterial and biological characteristics of silver containing and strontium doped plasma sprayed hydroxyapatite coatings. *Acta Biomater.* **2012**, *8*, 3144–3152. [[CrossRef](#)]
170. Vahabzadeh, S.; Roy, M.; Bandyopadhyay, A.; Bose, S. Phase stability and biological property evaluation of plasma sprayed hydroxyapatite coatings for orthopedic and dental applications. *Acta Biomater.* **2015**, *17*, 47–55. [[CrossRef](#)]
171. Singh, G.; Singh, S.; Prakash, S. Role of Post Heat Treatment of Plasma Sprayed Pure and Al₂O₃-TiO₂ Reinforced Hydroxyapatite Coating on the Microstructure and Mechanical Properties. *J. Miner. Mater. Charact. Eng.* **2010**, *9*, 1059–1069. [[CrossRef](#)]
172. Popa, M.V.; Moreno, J.M.C.; Popa, M.; Vasilescu, E.; Drob, P.; Vasilescu, C.; Drob, S.I.J.S.; Technology, C. Electrochemical deposition of bioactive coatings on Ti and Ti–6Al–4V surfaces. *Surf. Coat. Technol.* **2011**, *205*, 4776–4783. [[CrossRef](#)]
173. Chen, Y.M.; Lu, Y.P.; Li, M.S. Surface changes of plasma sprayed hydroxyapatite coatings before and after heat treatment. *Surf. Eng.* **2006**, *22*, 462–467. [[CrossRef](#)]
174. Sun, L.; Berndt, C.C.; Gross, K.A.; Kucuk, A. Material fundamentals and clinical performance of plasma-sprayed hydroxyapatite coatings: A review. *J. Biomed. Mater. Res.* **2001**, *58*, 570–592. [[CrossRef](#)]
175. Roy, M.; Balla, V.K.; Bose, S.; Bandyopadhyay, A. Comparison of Tantalum and Hydroxyapatite Coatings on Titanium for Applications in Load Bearing Implants. *Adv. Eng. Mater.* **2010**, *12*, B637–B641. [[CrossRef](#)]
176. Ke, D.; Vu, A.A.; Bandyopadhyay, A.; Bose, S. Compositionally graded doped hydroxyapatite coating on titanium using laser and plasma spray deposition for bone implants. *Acta Biomater.* **2019**, *84*, 414–423. [[CrossRef](#)]
177. Singh, G.; Singh, S.; Prakash, S. Surface characterization of plasma sprayed pure and reinforced hydroxyapatite coating on Ti6Al4V alloy. *Surf. Coat. Technol.* **2011**, *205*, 4814–4820. [[CrossRef](#)]
178. Li, H.; Khor, K.; Cheang, P. Titanium dioxide reinforced hydroxyapatite coatings deposited by high velocity oxy-fuel (HVOF) spray. *Biomaterials* **2002**, *23*, 85–91. [[CrossRef](#)]
179. Bolelli, G.; Giovanardi, R.; Lusvardi, L.; Manfredini, T. Corrosion resistance of HVOF-sprayed coatings for hard chrome replacement. *Corros. Sci.* **2006**, *48*, 3375–3397. [[CrossRef](#)]

180. Ban, Z.-G.; Shaw, L.L. Characterization of Thermal Sprayed Nanostructured WC-Co Coatings Derived From Nanocrystalline WC-18wt.%Co Powders. *J. Spray Technol.* **2003**, *12*, 112–119. [[CrossRef](#)]
181. Visai, L.; De Nardo, L.; Punta, C.; Melone, L.; Cigada, A.; Imbriani, M.; Arciola, C.R. Titanium Oxide Antibacterial Surfaces in Biomedical Devices. *Int. J. Artif. Organs* **2011**, *34*, 929–946. [[CrossRef](#)] [[PubMed](#)]
182. Song, B.; Pala, Z.; Voisey, K.; Hussain, T. Gas and liquid-fuelled HVOF spraying of Ni50Cr coating: Microstructure and high temperature oxidation. *Surf. Coat. Technol.* **2017**, *318*, 224–232. [[CrossRef](#)]
183. Heimann, R.B.; Lehmann, H.D. Deposition, Structure, Properties and Biological Function of Plasma-Sprayed Bioceramic Coatings. *Bioceram. Coat. Med. Implant.* **2015**, *6*, 253–308.
184. Yao, H.-L.; Wang, H.-T.; Bai, X.-B.; Ji, G.-C.; Chen, Q.-Y. Improvement in mechanical properties of nano-structured HA/TiO₂ multilayer coatings deposited by high velocity suspension flame spraying (HVSFS). *Surf. Coat. Technol.* **2018**, *342*, 94–104. [[CrossRef](#)]
185. Cotell, C.M.; Chrisey, D.B.; Grabowski, K.S. Pulsed Laser Deposition of Biocompatible Thin Films: Calcium Hydroxylapatite and Other Calcium Phosphates. *MRS Proc.* **1991**, *252*, 549. [[CrossRef](#)]
186. Suchanek, W.; Yoshimura, M. Processing and properties of hydroxyapatite-based biomaterials for use as hard tissue replacement implants. *J. Mater. Res.* **1998**, *13*, 94–117. [[CrossRef](#)]
187. Yang, Y.; Chang, E. Influence of residual stress on bonding strength and fracture of plasma-sprayed hydroxyapatite coatings on Ti-6Al-4V substrate. *Biomaterials* **2001**, *22*, 1827–1836. [[CrossRef](#)]
188. Zhao, Y.; Song, M.; Chen, C.; Liu, J. The role of the pressure in pulsed laser deposition of bioactive glass films. *J. Non-Cryst. Solids* **2008**, *354*, 4000–4004. [[CrossRef](#)]
189. Xiong, J.; Li, Y.; Hodgson, P.D.; Wen, C. Nanohydroxyapatite coating on a titanium–niobium alloy by a hydrothermal process. *Acta Biomater.* **2010**, *6*, 1584–1590. [[CrossRef](#)]
190. Ninomiya, J.T.; Struve, J.A.; Stelloh, C.T.; Toth, J.M.; Crosby, K.E. Effects of hydroxyapatite particulate debris on the production of cytokines and proteases in human fibroblasts. *J. Orthop. Res.* **2001**, *19*, 621–628. [[CrossRef](#)]
191. Ehrenfest, D.M.D.; Coelho, P.G.; Kang, B.S.; Sul, Y.T.; Albrektsson, T. Classification of osseointegrated implant surfaces: Materials, chemistry and topography. *Trends Biotechnol.* **2010**, *28*, 198–206. [[CrossRef](#)] [[PubMed](#)]
192. JONES, J.R. Scaffolds for tissue engineering. In *Biomaterials, Artificial Organs and Tissue Engineering*; Elsevier: Amsterdam, The Netherlands, 2005; pp. 201–214.
193. Nelea, V.; Morosanu, C.; Iliescu, M.; Mihailescu, I. Hydroxyapatite thin films grown by pulsed laser deposition and radio-frequency magnetron sputtering: Comparative study. *Appl. Surf. Sci.* **2004**, *228*, 346–356. [[CrossRef](#)]
194. Johnson, S. Pulsed laser deposition of hydroxyapatite thin films. *Mater. Sci. Eng. C* **2007**, *27*, 484–494.
195. Carradò, A. Nano-crystalline pulsed laser deposition hydroxyapatite thin films on Ti substrate for biomedical application. *J. Coat. Technol. Res.* **2011**, *8*, 749–755. [[CrossRef](#)]
196. Rau, J.V.; Cacciotti, I.; Laureti, S.; Fosca, M.; Varvaro, G.; Latini, A. Bioactive, nanostructured Si-substituted hydroxyapatite coatings on titanium prepared by pulsed laser deposition. *J. Biomed. Mater. Res. Part. B Appl. Biomater.* **2015**, *103*, 1621–1631. [[CrossRef](#)]
197. Liu, Y.-C.; Lin, G.S.; Wang, J.-Y.; Cheng, C.-S.; Yang, Y.-C.; Lee, B.-S.; Tung, K.-L. Synthesis and characterization of porous hydroxyapatite coatings deposited on titanium by flame spraying. *Surf. Coat. Technol.* **2018**, *349*, 357–363. [[CrossRef](#)]
198. Guo, D.; Li, F.; Wang, J.; Sun, J. Effects of post-coating processing on structure and erosive wear characteristics of flame and plasma spray coatings. *Surf. Coat. Technol.* **1995**, *73*, 73–78. [[CrossRef](#)]
199. Yang, Y.-C.; Chen, C.-C.; Wang, J.-B.; Wang, Y.-C.; Lin, F.-H. Flame sprayed zinc doped hydroxyapatite coating with antibacterial and biocompatible properties. *Ceram. Int.* **2017**, *43*, S829–S835. [[CrossRef](#)]
200. Sun, L.; Berndt, C.C.; Gross, K.A. Hydroxyapatite/polymer composite flame-sprayed coatings for orthopedic applications. *J. Biomater. Sci. Polym. Ed.* **2002**, *13*, 977–990. [[CrossRef](#)]
201. Antala, N.; Rathod, P. A Review of the Coating Characteristics Achieved Employing Thermal Flame-spray Coating Method. *Int. J. Eng. Technol. Manag. Appl. Sci.* **2017**, *5*.
202. Zheng, X.; Huang, M.; Ding, C. Bond strength of plasma-sprayed hydroxyapatite/Ti composite coatings. *Biomaterials* **2000**, *21*, 841–849. [[CrossRef](#)]
203. Mumith, A.; Cheong, V.S.; Fromme, P.; Coathup, M.J.; Blunn, G.W. The effect of strontium and silicon substituted hydroxyapatite electrochemical coatings on bone ingrowth and osseointegration of selective laser sintered porous metal implants. *PLoS ONE* **2020**, *15*, e0227232. [[CrossRef](#)] [[PubMed](#)]

204. Ullah, I.; Siddiqui, M.A.; Liu, H.; Kolawole, S.K.; Zhang, J.; Zhang, S.; Ren, L.; Yang, K. Mechanical, Biological, and Antibacterial Characteristics of Plasma-Sprayed (Sr, Zn) Substituted Hydroxyapatite Coating. *ACS Biomater. Sci. Eng.* **2020**, *6*, 1355–1366. [[CrossRef](#)]
205. Zieliński, A.; Antoniuk, P.; Krzysztofowicz, K. Nanotubular oxide layers and hydroxyapatite coatings on 'Ti-13Zr-13Nb' alloy. *Surf. Eng.* **2014**, *30*, 643–649. [[CrossRef](#)]
206. Vu, A.A.; Robertson, S.F.; Ke, D.; Bandyopadhyay, A.; Bose, S. Mechanical and biological properties of ZnO, SiO₂, and Ag₂O doped plasma sprayed hydroxyapatite coating for orthopaedic and dental applications. *Acta Biomater.* **2019**, *92*, 325–335. [[CrossRef](#)]
207. Furko, M.; Havasi, V.; Kónya, Z.; Grünewald, A.; Detsch, R.; Boccaccini, A.R.; Balázs, C. Development and characterization of multi-element doped hydroxyapatite bioceramic coatings on metallic implants for orthopedic applications. *Bol. De La Soc. Española De Ceram. Y Vidr.* **2018**, *57*, 55–65. [[CrossRef](#)]
208. Kurzweg, H.; Heimann, R.; Troczynski, T.; Wayman, M. Development of plasma-sprayed bioceramic coatings with bond coats based on titania and zirconia. *Biomaterials* **1998**, *19*, 1507–1511. [[CrossRef](#)]
209. Jung, U.-W.; Hwang, J.-W.; Choi, D.-Y.; Hu, K.-S.; Kwon, M.-K.; Choi, S.-H.; Kim, H.-J. Surface characteristics of a novel hydroxyapatite-coated dental implant. *J. Periodontal Implant. Sci.* **2012**, *42*, 59–63. [[CrossRef](#)]
210. Jia, L.; Liang, C.; Huang, N.; Duan, F.; Wang, L. Formation of Hydroxyapatite Produced by Microarc Oxidation Coupled with Sol-gel Technology. *Mater. Manuf. Process.* **2014**, *29*, 1085–1094. [[CrossRef](#)]
211. Li, L.-H.; Kim, H.-W.; Lee, S.-H.; Kong, Y.-M.; Kim, H.-E. Biocompatibility of titanium implants modified by microarc oxidation and hydroxyapatite coating. *J. Biomed. Mater. Res. Part. A* **2005**, *73*, 48–54. [[CrossRef](#)]
212. Jin, Y.-Z.; Zheng, G.-B.; Jang, H.L.; Lee, K.M.; Lee, J.H. Whitlockite Promotes Bone Healing in Rabbit Ilium Defect Model. *J. Med. Biol. Eng.* **2019**, *39*, 944–951. [[CrossRef](#)]
213. Batool, S.; Liaqat, U.; Hussain, Z.; Sohail, M. Synthesis, Characterization and Process Optimization of Bone Whitlockite. *Nanomaterials* **2020**, *10*, 1856. [[CrossRef](#)] [[PubMed](#)]
214. Zhou, D.; Qi, C.; Chen, Y.-X.; Zhu, Y.-J.; Sun, T.-W.; Chen, F.; Zhang, C. Comparative study of porous hydroxyapatite/chitosan and whitlockite/chitosan scaffolds for bone regeneration in calvarial defects. *Int. J. Nanomed.* **2017**, *12*, 2673–2687. [[CrossRef](#)] [[PubMed](#)]

Publisher's Note: MDPI stays neutral with regard to jurisdictional claims in published maps and institutional affiliations.



© 2020 by the authors. Licensee MDPI, Basel, Switzerland. This article is an open access article distributed under the terms and conditions of the Creative Commons Attribution (CC BY) license (<http://creativecommons.org/licenses/by/4.0/>).